KIM223EL INORGANIC CHEMISTRY LABORATORY

KIM 223EL

Inorganic Chemistry

Manual of Laboratory Experiments

Prof. Dr. Zehra Bayır

Prof. Dr. Ozan Sanlı Şentürk

February, 2023

Istanbul Technical University

Department of Chemistry

Laboratory of Inorganic Chemistry

34469 Maslak, Istanbul

Preface

This booklet is designed for your Inorganic Chemistry Laboratory lectures and we hope that you will find it useful in the course.

The experiments range from Schiff's bases to molecular modeling, VSEPR theory, Werner-type complexes, chromium chemistry, bioinorganic chemistry and modeling, chelate complexes, magnetic phenomena in inorganic chemistry, and spectroscopy.

We tried to include the most modern concepts of inorganic chemistry in these laboratory lectures and we hope the outcome is useful for everybody.

CONTENTS

1	***NICKEL COMPLEX OF A SCHIFF'S BASE***	**1.1**
	Special Security Precautions	**1.2**
	General Information	**1.3**
	Experimental Section	2 1.3.1
	Preparation of the Schiff's Base	2
1.3.2	Preparation of the Transition Metal Complexes	2
1.3.3	Helpful information for metal complex formation	3
1.4	**Preparation of the assignment**	**3 1.5**
	References	**3 *2***
	STRUCTURAL CHARACTERIZATION IN INORGANIC CHEMISTRY	**5 2.1**
	Single Crystal X-Ray Analysis	6 2.1.1
	Single-crystal X-ray Diffraction Instrument	6
2.1.2	What is the Crystal?	7
2.1.3	Lattice and Crystal Systems	9
2.2	**Nuclear Magnetic Resonance (NMR) Spectroscopy**	**11 2.2.1**
	Principle of Nuclear Magnetic Resonance NMR Spectroscopy	11
2.2.2	Working of Nuclear Magnetic Resonance (NMR) Spectroscopy	12
2.2.3	Electronic density	12
2.3	**Infrared (IR) Spectroscopy**	**13 2.3.1**
	The shape of peaks in the IR spectrum	14
2.4	**Preparation of the assignment**	**17 *3***
	THE VSEPR THEORY	**19 3.1**
	Basic Assumptions	**19 3.2**
	AXE Method	**20 3.3**
	Examples	**20 3.4**
	Symmetry Elements and Operations	23 3.4.1
	Introduction	23
3.4.2	Symmetry Elements and Operations	23
3.4.3	POINT GROUPS	31
3.4.4	Examples of the Impact of Geometric Symmetry on Chemistry	31
3.4.5	Infrared Spectroscopy	32
3.4.6	Nuclear Magnetic Resonance: Chemical Equivalence	33
3.4.7	Self-Test Questions	38
3.5	**References**	**38 *4***
	POTASSIUM BIS(OXALATO)CUPRATE(II) DIHYDRATE: PREPARATION AND ANALYSIS	**39 4.1**
	Theory	**39 4.2**
	Chemicals	**39 4.3**
	Glassware	**39 4.4**
	Preparation of potassium bis(oxalato)cuprate(II) dihydrate	**40 4.5**
	Determination of the oxalate content	**40 4.6**
	Determination of the copper content	**40 4.7**
	Determination of the hydrate content	**41 4.8**
	Qualitative work	**41 4.9**
	Treatment of data	**41 4.10**
	References	**42 *5***
	PREPARATION AND INVESTIGATION OF SOME COORDINATION COMPOUNDS	**43 5.1**
	Special Safety Precautions	**43 5.2**
	Experimental	43 5.2.1
	Instructions for Course Organisers	43

5.2.2 Hexaamminenickel(ll) tetrafluoroborate $[Ni(NH_3)_6](BF_4)_2$, 43
5.2.3 Potassium Tris(oxalato)ferrate(III) 44
5.3 Chemical Properties 445.3.1
Thermal decomposition of hexaamminenickel(II) tetrafluoroborate 45
5.4 Reference 45***6***
SIMULATION OF ATOMIC AND MOLECULAR ORBITALS 45**6.1**
Purpose 47**6.2**
General Information 47**6.3**
Procedure 49**6.4**
Experimental 506.4.1
Materials required 50
6.4.2 The 1s atomic orbital 51
6.4.3 The 2p atomic orbital 51
6.4.4 The 3d atomic orbital 51
6.4.5 Nodes 52
6.4.6 σ (1s) orbital in H_2 52
6.4.7 π and π* orbitals in ethene 52
6.4.8 P-O π-bonding in $OPCl_3$ 53
6.4.9 Back-bonding in transition-metal carbonyls 53
6.4.10 Back-bonding in transition-metal ethene complexes 53
6.4.11 The π molecular orbitals in benzene 53
6.5 Exercises 54**6.6**
References 54***7***
METAL ACETYLACETONATE COMPLEXES: PREPARATION AND CHARACTERISATION 55**7.1**
Metal Acetylacetonates 567.1.1
Al^{3+} Complex 56
7.1.2 VO^{2+} complex 57
7.1.3 Cr^{3+} complex 57
7.1.4 Fe^{3+} complex 58
7.1.5 Co^{3+} complex 58
7.1.6 Cu^{2+} complex 58
7.2 Nuclear Magnetic Resonance Spectra of Acetyl Acetonates 59***8***
SPECTROPHOTOMETRIC DETERMINATION OF THE COMPOSITION OF A COORDINATION COMPLEX IN SOLUTION 63**8.1**
Ultraviolet-Visible (UV-Vis) Spectroscopy 63**8.2**
UV-Vis absorption bands 64**8.3**
Terminology 66**8.4**
Electronic Transitions 668.4.1
σ to σ * Transitions 67
8.4.2 n to σ * Transitions 67
8.4.3 n to π * and π to π * Transitions 67
8.5 Job's Method 67**8.6**
Experimental 698.6.1
Determination of the Composition of Fe+3- Salicylic Acid Complex 69
8.7 References 69

1 NICKEL COMPLEX OF A SCHIFF'S BASE

1.1 Special Security Precautions

Some chemicals used in this experiment are harmful by inhalation and by contact to skin, so bring rubber gloves and laboratory goggles. If your skin is affected, immediately wash with plenty of water and seek medical advice. If some chemicals are spilled into the fume hood, inform your assistant, wash the area with plenty of water, and drive the fluid into the hood's water outlet. The diamine compound used in our experiment gives out harmful fumes, so take the specimen inside a fume hood with fan running.

1.2 General Information

Schiff's bases are compounds formed after a condensation between a primary amine and an aldehyde/ketone with production of at least 1 mole of water (See Equation 1). The reaction can be repeated with quite a high number of substituents, but the reaction only proceeds with an aldehyde or a ketone with a primary amine.

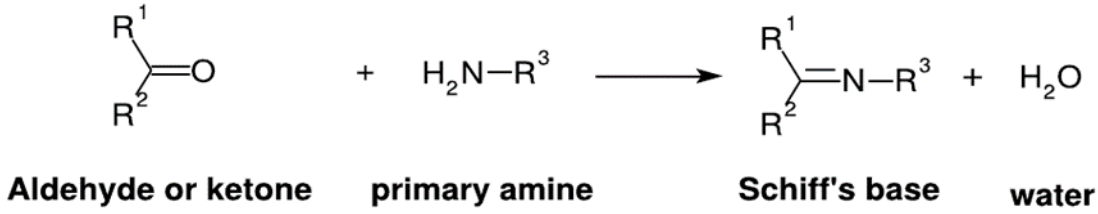

Figure 1.1: Formation of a Schiff's base between a carbonyl compound and a primary amine.

Equation 1 shows an aldehyde (R^1 or R^2 = H) or a ketone (R^1 and R^2 might be different or same and they are not H) reacting with a primary amine to form a Schiff's base with water as the second product in the reaction. If an aldehyde is used in the process, the formed Schiff's base can also be named as “aldimine”; similarly, “ketimine” is used for the Schiff's bases which were formed from a ketone. We have reviewed two requirements for a Schiff's base to form; an additional third requirement is that the pH value of the medium is around 4-5, enabling the protonation of the carbonyl compound. This is mostly supplied by conducting the reaction in ethyl alcohol, whose pH is around 4-5.

Schiff's bases are, from a coordination chemical background, Lewis' bases; the reason

behind this is the presence of a lone electron pair residing on the nitrogen atom. With suitable Lewis' acids, which have orbital voids to accept the lone pair electron, they can form Lewis' salts or metal complexes.

The first known instance of Schiff's base complexes were reported by Ettling in 1840. He synthesised the copper complex of a Schiff's base formed between salicylaldehyde and ammonia. However, the name Schiff's base was originated due to the studies by Hugo Schiff, because he managed to identify the metal/ligand ratio of the complex Ettling isolated to be 1:2 in the year 1869.

Schiff's base complexes play an important role in the development of modern coordination chemistry as coenzyme Vitamin B_{12} and haemin (the active part in haemoglobin) model compounds and some transition metal catalysts.

1.3 Experimental Section

1.3.1 Preparation of the Schiff's Base

Hint: It is more comfortable to work with volumes than with weights; so use the density information on the reagent bottles to convert to volumes.

Salicylaldehyde (2.44 g, 0.02 mol) is mixed with 15 mL of ethyl alcohol and 1.24 g (0.01 mol) of 1,3-diaminopropane. The resulting yellowish solution is refluxed for 35-40 minutes. After this time, a small amount of tap water is added to obtain a turbid appearance or a slight precipitate. In 1-2 days, crystallisation is observed and the crystals are transferred to a beaker for future use.

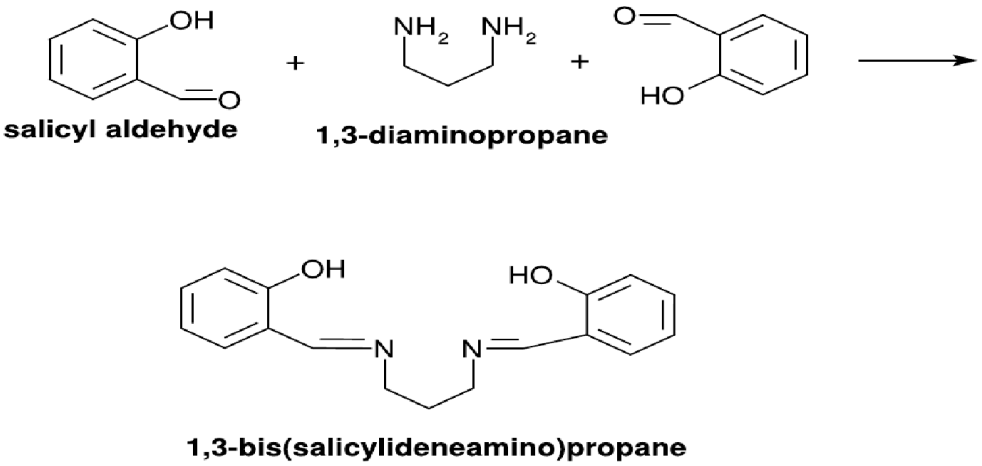

Figure 1.2: Formation of the Schiff's base between an aldehyde and a primary amine.

1.3.2 Preparation of the Transition Metal Complexes

Find a nickel salt (nickel chloride or nickel acetate will do) and according to the amount you are taking for complexation, find the amount of the nickel salt by 1:1 molar ratio. Obtain

two beakers with about 100-250 mL capacity and put the ligand you are using on one and put a little ethyl alcohol and the nickel salt on another, and add a little ethanol again. Use a hotplate to gently boil the alcohol and cool, you will probably have a different shade of green, which means that you have synthesised the nickel complex of the Schiff's base.

1.3.3 Helpful information for metal complex formation

There are some rules for metal complex formation. 1) If there are acidic hydrogens (carboxylic acid, phenol, thiol, etc) in the ligand, they will be dissociated in the complex to make negative charges. 2) The coordination number for a given metal is **always** completed by using the donor groups in the Schiff's base and auxilary ligands. 3) The positive charge is, if possible, neutralised by the donor groups to be 0. If not, as is the case for bis(ethylenediamine)copper (II), cationic or anionic complexes will result.

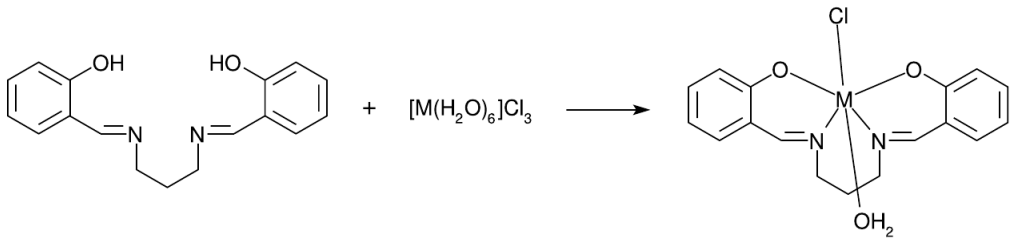

Formation of the metal complex between an aqueous solution of a trivalent metal chloride and 1,3-bis(salicylideneamino)propane

Figure 1.3: Formation of the metal complex between a ligand of a Schiff's base and a metal salt.

1.4 Preparation of the assignment

On the assignment, briefly mention of the historical perspectives of the Schiff's bases, with a slight emphasis to the Hugo Schiff's biography. Then write the synthetic part, using the numerical values and relevant calculation.

1.5 References

1. J.D. Woollins (ed), Inorganic Experiments, VCH, Weinheim, 1994.

2 STRUCTURAL CHARACTERIZATION IN INORGANIC CHEMISTRY

All substances around us consist of atoms. The types of atoms and their three-dimensional arrangement define the structure of materials, therefore the nature of materials. Since the properties and functions of materials relate directly to its structure, there exist extensive researches for various materials such as semiconductor, electronic, food, pharmaceutical, or life science related materials.

However, we can't recognize the structure of materials at the atomic level because of the limited resolution mainly due to the wavelength, as long as we see objects with our eyes by using visible light. For example, we neither can distinguish a grain of table salt from that of sugar by their atomic level structures, nor can have a clear view of the turtle shell-shaped 6-membered rings (benzene rings) by just staring at the medicine for colds.

Recently, elucidation of molecular structures is becoming more common owing to the developments of various measurement techniques (See Table 2.1). Nuclear magnetic resonance (NMR), mass spectrometry (MS), and infrared spectroscopy (IR) are the typical examples. However, these spectroscopic techniques derive just a list of partial structures, and it is sometimes difficult to deduce the three-dimensional structure of a whole molecule. On the other hand, it is the molecular structure itself that is derived from the single crystal X-ray analysis (SCXRD). The single crystal analysis provides a unanimous conclusion that sometimes puts an end to arguments over molecular or crystal structures.

Table 2.1. Comparison between characterization methods

	SCXRD	NMR	MS	IR
Nondestructive measurement	○	○	×	○
Sample form	Crystal	Liquid Solid	Solid Liquid Gas	Solid Liquid Gas
Measurable atomic types	All	Limited	All	All
Determination of configuration	○	○ (Indirect)	×	×
Determination of absolute structure	○	△ (Indirect)	×	×
Determination of crystal strcutre	○	×	×	×
Sample preparation	Difficult	Middle	Easy	Easy
Data interpretation	Direct	Indirect	Indirect	Indirect

SCXRD: single crystal X-ray analysis
NMR: nuclear magnetic resonance
MS: mass spectrometry
IR: infrared spectroscopy

2.1 Single Crystal X-Ray Analysis

Single-crystal X-ray Diffraction is a non-destructive analytical technique which provides detailed information about the internal lattice of crystalline substances, including unit cell dimensions, bond-lengths, bond-angles, and details of site-ordering. Directly related is single-crystal refinement, where the data generated from the X-ray analysis is interpreted and refined to obtain the crystal structure.

The history of crystallography starts with the discovery of X-rays in 1895 by Wilhelm Conrad Röntgen whose name is used as a synonym of the X-ray photography in the medical field. In 1912, Max von Laue observed of the fist X-ray diffraction pattern from the copper sulfate crystal. Next year, William Lawrence Bragg and his father William Henry Bragg discovered the Bragg's law that makes it possible to calculate the positions of the atoms. In the 1910s, the structures of inorganic materials including sodium chloride, mineral and diamond were determined by the X-ray crystallography. The single crystal analysis was first applied to physics and chemistry.

2.1.1 Single-crystal X-ray Diffraction Instrument

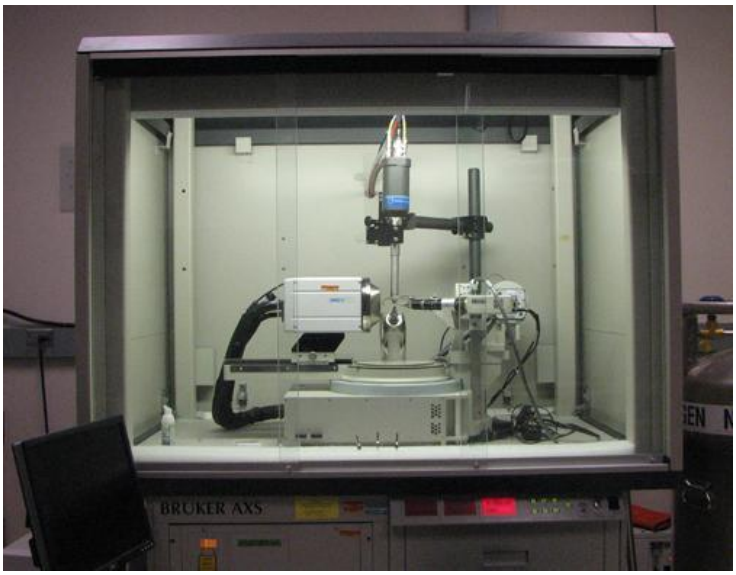

Figure 2.1: Single-crystal X-ray diffraction instrument.

X-ray diffractometers consist of three basic elements, an X-ray tube, a sample holder, and an X-ray detector. X-rays are generated in a cathode ray tube by heating a filament to produce electrons, accelerating the electrons toward a target by applying a voltage, and impact of the electrons with the target material. When electrons have sufficient energy to dislodge inner shell electrons of the target material, characteristic X-ray spectra are produced. These

spectra consist of several components, the most common being Kα and Kβ. Kα consists, in part, of Kα1 and Kα2. Kα1 has a slightly shorter wavelength and twice the intensity as Kα2. The specific wavelengths are characteristic of the target material. Filtering, by foils or crystal monochrometers, is required to produce monochromatic X-rays needed for diffraction. Kα1and Kα2 are sufficiently close in wavelength such that a weighted average of the two is used. Molybdenum is the most common target material for single-crystal diffraction, with MoKα radiation = 0.7107Å. These X-rays are collimated and directed onto the sample. When the geometry of the incident X-rays impinging the sample satisfies the Bragg Equation, constructive interference occurs. A detector records and processes this X-ray signal and converts the signal to a count rate which is then output to a device such as a printer or computer monitor. X-rays may also be produced using a synchotron, which emits a much stronger beam.

Figure 2.2: Single-crystal X-ray diffraction instrument.

Single-crystal diffractometers use either 3- or 4-circle goniometers. These circles refer to the four angles (2θ, χ, φ, and Ω) that define the relationship between the crystal lattice, the incident ray and detector. Samples are mounted on thin glass fibers which are attached to brass pins and mounted onto goniometer heads. Adjustment of the X, Y and Z orthogonal directions allows centering of the crystal within the X-ray beam.

2.1.2 What is the Crystal?

A single crystal, also called monocrystal, is a crystalline solid in which the crystal lattice of the entire sample is continuous and unbroken to the edges of the sample, with no grain boundaries. For viewing the three-dimensional structure of molecules quantitatively, it is required to satisfy the following three conditions.

1) Types of atoms are distinguishable

2) The position of the individual atom which is buried inside of the molecule can be determined even if the molecule is large like proteins
3) The view of molecules from as many different directions as possible can be obtained. In addition, the relative positions among the molecules from different view can be determined precisely.

X-ray crystallography gives a black dotted image as shown in Figure 3. When parallel X-rays irradiate an object, only shadow image is projected on the screen. At the same time, most of the X-rays are reflected similar to visible light. It is called scattered X-rays. Scattered X-rays induce the phenomenon of coherent interference because X-rays can be thought as waves, and result in X-ray diffraction. If the object is a crystal, X-ray diffraction forms diffraction spots to the specific directions on the screen (black dots shown in Fig. 2.3). Each diffraction spot carries contribution from all atoms in the original object, and it is necessary to collect all diffraction spots to recreate the real image. The information about the positions and the intensities of diffraction spots is recorded on the screen, so-called a "detector". As shown in Fig. 4, based on the positions and the intensities of collected diffraction pattern, electron density distributions in crystals can be obtained after the calculation corresponding to the lenses in the microscope. X-ray crystallography assumes that atoms are present at the electron density maxima. Determination of positions of atoms, or atomic coordinates, results in a molecular model.

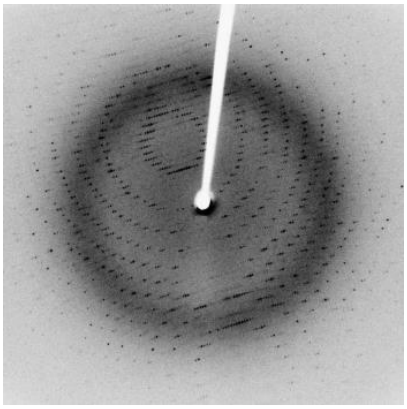

Figure 2.3: X-ray diffraction pattern of single crystal.

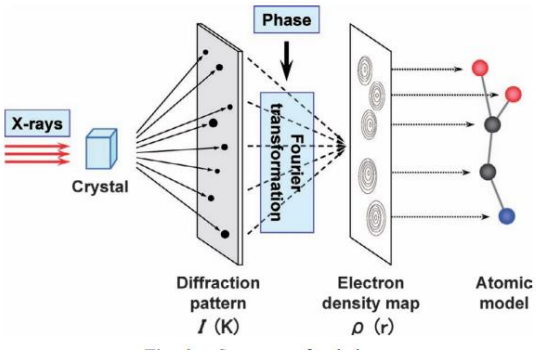

Figure 2.4: Summary of technique.

2.1.3 Lattice and Crystal Systems

Crystals can be classified into 32 point groups on the basis of eight kinds of symmetry elements. There are seven crystal systems for classification, which consist of 14 kinds of Bravais lattices. For convenience, these relations are illustrated in Fig. 2.5. Furthermore, if it is extended to include space groups, by adding point groups, Bravais lattices, screw axis, and glide reflection axis, there will be 230 classifications in total. In other words, all crystals "belong to one of 230 space groups," the details available in other books on crystallography (see for example International Tables for X-ray Crystallography published by the International Union of Crystallography).

By putting lattice points at the corner of these crystal systems for finding a certain minimum set of symmetry elements, seven kinds of crystal systems are obtained as shown in Table 2. That is, only seven different kinds of cells are necessary to cover all possible point lattices or all crystals can be classified into one of the seven crystal systems. Nevertheless, there are other ways for fulfilling the condition that each point has identical surroundings. In this regard, Auguste Bravais (physicist in France) found that there are 14 possible point lattices and no more and we use e Bravais lattices as shown in Fig. 2.6.

Table 2.2. Summary of seven crystal systems and Bravais lattices

System	Axial lengths and angles	Bravais lattice	Lattice symbol
Cubic	Three equal axes at right angles $a = b = c, \alpha = \beta = \gamma = 90°$	Simple	P
		Body-centered	I
		Face-centered	F
Tetragonal	Three axes at right angles, two equals $a = b \neq c, \alpha = \beta = \gamma = 90°$	Simple	P
		Body-centered	I
Orthorhombic	Three unequal axes at right angles $a \neq b \neq c, \alpha = \beta = \gamma = 90°$	Simple	P
		Body-centered	I
		Base-centered	C
		Face-centered	F
Trigonal*	Three equal axes, equally inclined $a = b = c, \alpha = \beta = \gamma \neq 90°$	Simple	R
Hexagonal	Two equal coplanar axes at, 120° third axis at right angles $a = b \neq c, \alpha = \beta = 90°, \gamma = 120°$	Simple	P
Monoclinic	Three unequal axes, one pair not at right angles $a \neq b \neq c$, $\alpha \neq \gamma = 90° \neq \beta$	Simple	P
		Base-centered	C
Triclinic	Three unequal axes, unequally inclined and none at right angles $a \neq b \neq c, \alpha \neq \beta \neq \gamma \neq 90°$	Simple	P

*Also called rhombohedral.

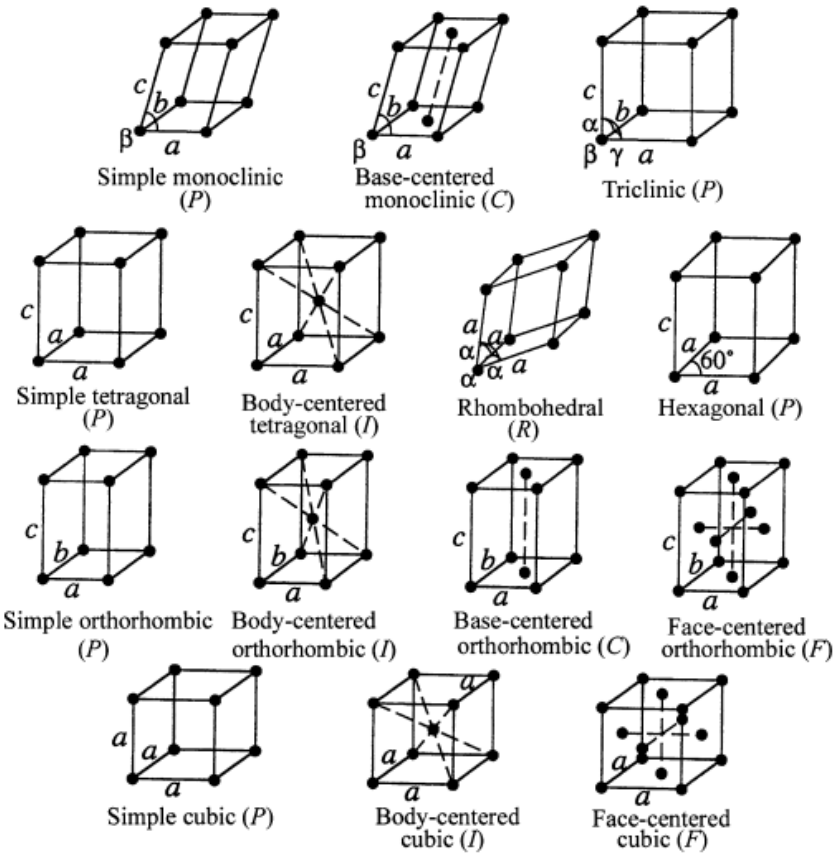

Figure 2.6: The fourteen Bravais lattices

2.2 Nuclear Magnetic Resonance (NMR) Spectroscopy

Nuclear magnetic resonance (NMR) spectroscopy has been developed to be the most powerful analytical method. It allows the visualisation of single atoms and molecules in various media in solution as well as in solid state. NMR is non-destructive and gives molar response that allows structure elucidation and quantification simultaneously.

The steady progress of NMR spectroscopy can clearly be seen in the list of Noble Prize winners. In 1944 the first Nobel Prize in physics was awarded to Rabi for the development of a resonance method that enables recording of the magnetic properties of atomic nuclei.

2.2.1 Principle of Nuclear Magnetic Resonance NMR Spectroscopy

It is a spectroscopy technique that is based on the absorption of electromagnetic radiation in the radiofrequency region 4 to 900 MHz by nuclei of the atoms. Over the past fifty years, NMR has become the preeminent technique for determining the structure of organic compounds. Of all the spectroscopic methods, it is the only one for which a complete analysis and interpretation of the entire spectrum is normally expected.

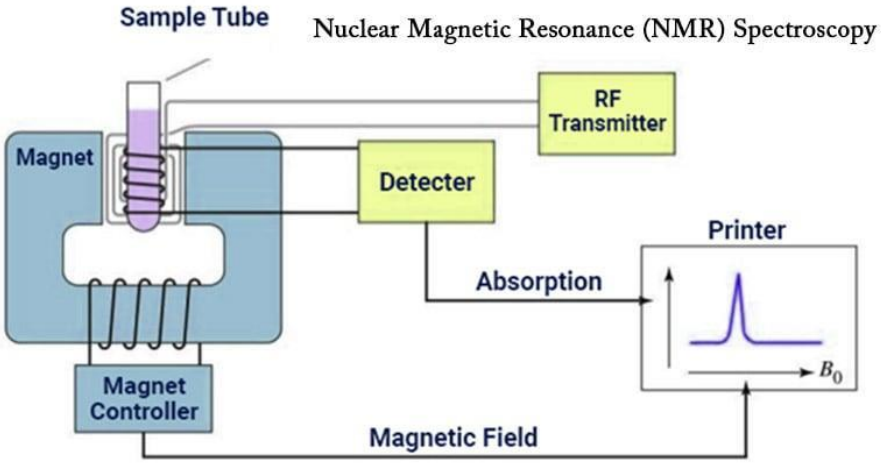

Figure 2.7: Nuclear magnetic resonance spectroscopy.

1) The principle behind NMR is that many nuclei have spin and all nuclei are electrically charged. If an external magnetic field is applied, an energy transfer is possible between the base energy to a higher energy level (generally a single energy gap).
2) The energy transfer takes place at a wavelength that corresponds to radio frequencies and when the spin returns to its base level, energy is emitted at the same frequency.
3) The signal that matches this transfer is measured in many ways and processed in order to yield an NMR spectrum for the nucleus concerned.

2.2.2 Working of Nuclear Magnetic Resonance (NMR) Spectroscopy

- The sample is placed in a magnetic field and the NMR signal is produced by excitation of the nuclei sample with radio waves into nuclear magnetic resonance, which is detected with sensitive radio receivers.
- The intramolecular magnetic field around an atom in a molecule changes the resonance frequency, thus giving access to details of the electronic structure of a molecule and its individual functional groups.
- As the fields are unique or highly characteristic to individual compounds, NMR spectroscopy is the definitive method to identify monomolecular organic compounds.
- Besides identification, NMR spectroscopy provides detailed information about the structure, dynamics, reaction state, and chemical environment of molecules.
- The most common types of NMR are proton and carbon-13 NMR spectroscopy, but it is applicable to any kind of sample that contains nuclei possessing spin.

2.2.3 Electronic density

Each atom is surrounded by electrons. The same kind of atom can generate signals with different chemical shift values. These chemical shifts differ as the magnetic field sensed by a particular nucleus strongly depends on its local chemical environment. The circulation of electrons in the surroundings of a nucleus creates small magnetic fields that oppose the applied external field. This "shielding" effect (σ) is directly proportional to the electronic density around the nucleus. Therefore, in NMR spectroscopy, upfield and downfield are terms that refer to the regions of lower and higher values, respectively, within the chemical shift scale.

The chemical shift scale in an NMR spectrum is represented from right to left. The zero value is established using a standard compound whose carbon and hydrogen atoms are strongly shielded and hence, their signals appear in the furthest upfield region (Figure 2.8). The assignment of the NMR spectra is usually performed with the help of NMR charts or diagrams that facilitate the identification of the NMR signals.

Hydrogens or carbons that are highly shielded, such as the ones of methyl groups, have low chemical shift values. However, hydrogens attached to very electronegative groups (e.g., carboxylic acids, ketones or aldehydes) have high chemical shift values (Figures 2.8 and 2.9).

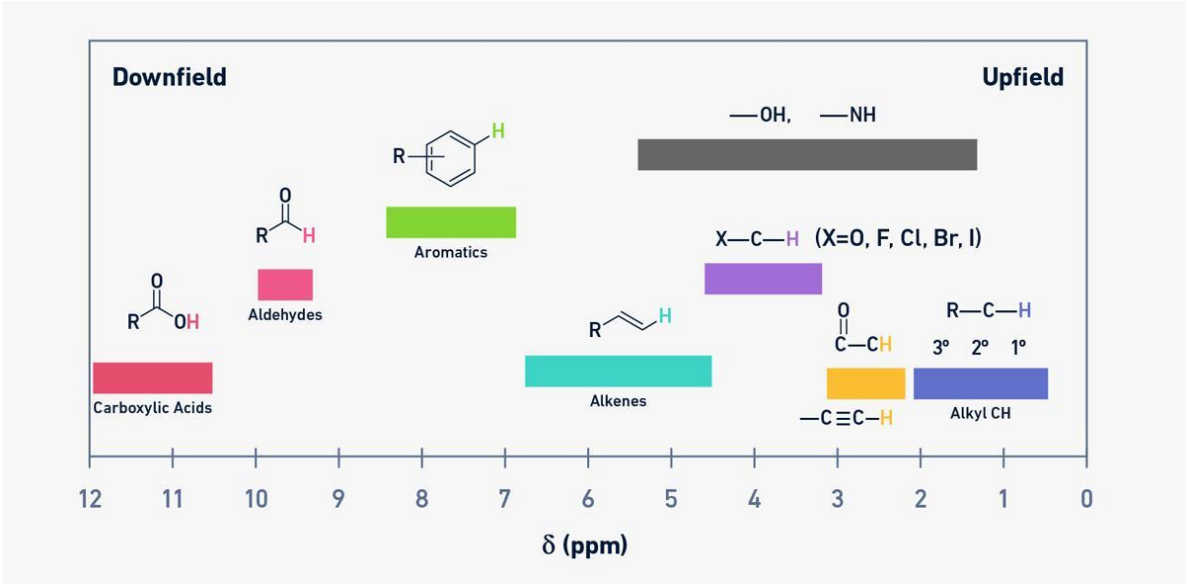

Figure 2.8: ^{1}H NMR chemical shift

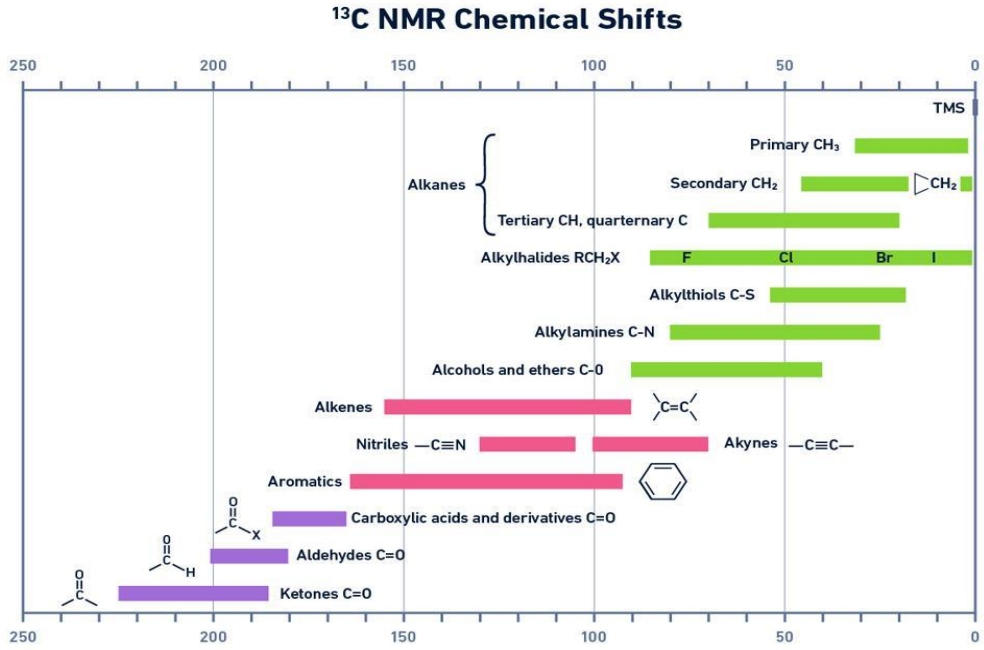

Figure 2.9: ^{13}C NMR chemical shift

2.3 Infrared (IR) Spectroscopy

All the spectroscopic methods, except mass spectrometry, can be classified according

to the energy involved during measurement. Electromagnetic radiation, of which visible light forms a tiny part, exists as waves that are propagated from a source and move in a straight line if they are not reflected or refracted. The undulatory phenomenon is a magnetic field associated with an electric one. The speed of the electromagnetic wave is a universal constant "c," equal to 3×10^{8} m/s.

The mid-infrared (MIR) region (2500–25000 nm or 4000–400 cm^{-1}) is the main region of vibrational spectroscopy. This region retains information, allowing organic molecules to be identified and the structure and conformation of molecules such as proteins, polysaccharides, and lipids to be characterized. In general, the absorption of an infrared radiation corresponds to an energy change ranging between 2 and 10 kcal mol^{-1}.

In IR spectrometry, electromagnetic radiation stimulates the vibration and rotational levels of molecules. Vibration and amplitudes increase depending on the mass of the molecule, the strength of the bonds, and the geometry of the molecule.

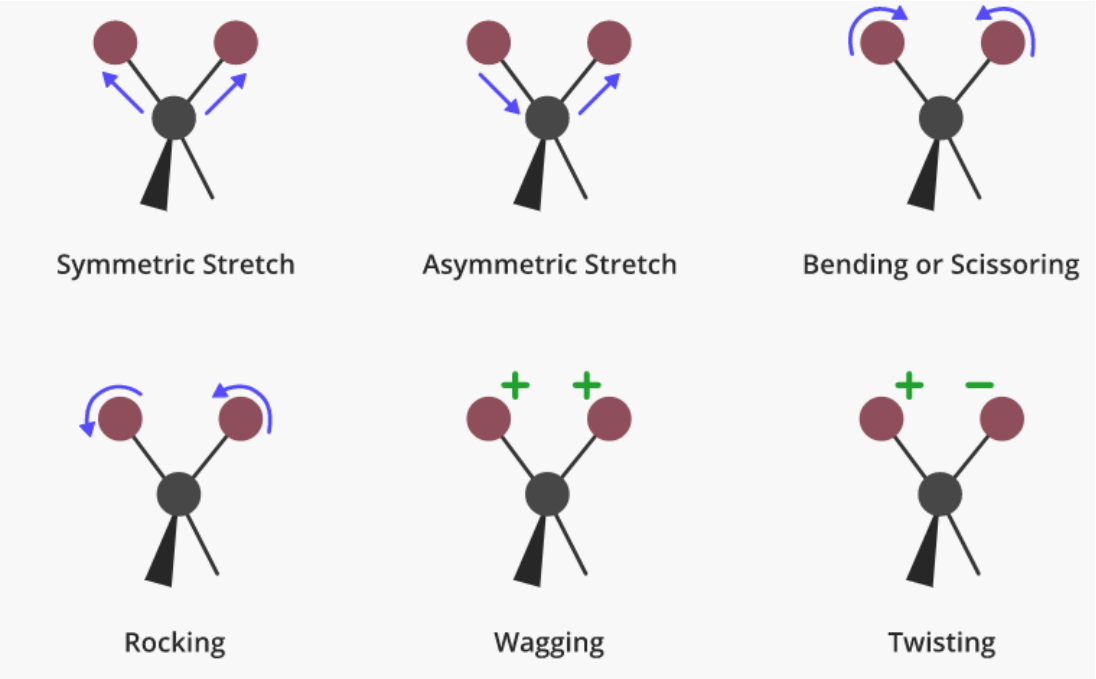

Figure 2.10: Molecular vibrations to infrared radiations.

2.3.1 The shape of peaks in the IR spectrum

Infrared absorptions are primarily visible as broad peaks on the graph. The broadening is caused by the doppler effect. The second broadening is caused by the collision between the molecules.

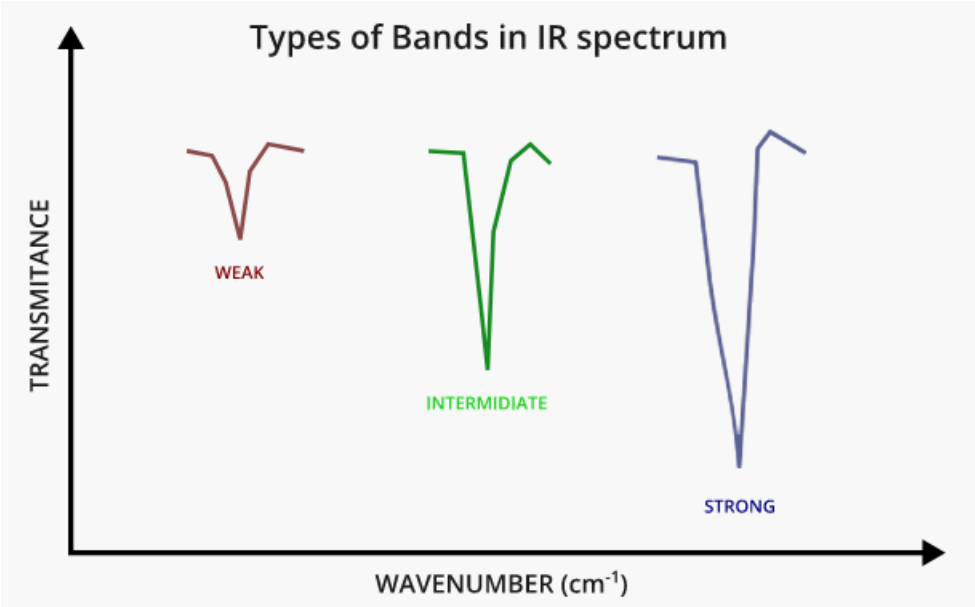

Figure 2.11: Types of Bands in IR Spectrum

Absorption occurs only when a vibration with particular energy changes a molecular's dipole moment. The larger the change in the dipole moment, the more intense the absorption band.

Table 2.2. IR spectrum table.

Bond	**Functional Group**	**Frequency in cm^{-1} (Intensity*)**
C–H	**Alkane**	3000–2850 (s)
	–CH_3	1450 and 1375 (m)
	–CH_2–	1465 (m)
	Alkene	3100–3000 (m), 1000–650 (s)
	Aromatic	3100–3050 (s), 900–690 (s)
	Alkyne (terminal)	3300 (s)

	Aldehyde	2850 and 2750 (w)
C=C	**Alkene**	1630 (w-m)
	Aromatic	1600–1475 (w-m)
C–C	**Alkyne**	2150–2100 (w-m)
C=O	**Aldehyde**	1740–1720 (s)
	Ketone	1725–1705 (s)
	Carboxylic Acid	1730–1700 (s)
	Ester	1750–1730 (s)
	Amide	1670–1640 (s)
	Anhydride	1810 and 1760 (s)
	Acid Chloride	1800 (s)
C–O	**Alcohol, Ether, Ester, Carboxylic Acid, Anhydride**	1300–1000 (s)
O–H	**Alcohol, Phenol**	
	Free	3650–3600 (m)
	Hydrogen-bonded	3500–3200 (m)
	Carboxylic Acids	3300–2400 (m)

N–H	**Primary and Secondary Amine and Amide**	3550–3060 (m-s); 1640–1550 (m-s)
C–N	**Amine**	1250–1000 (m-s)
C=N	**Imine and Oxime**	1690–1640 (w-s)
C=N	**Nitrile**	2260–2240 (m)
N=O	**Nitro (R–NO_2)**	1550 and 1350 (s)
C–Cl	**Chloride**	800–600 (s)

s = strong; m = medium; w = weak

2.4 Preparation of the assignment

On the assignment, briefly write the working principle of IR, NMR and SCXRD devices. Then write the estimated ^{1}H NMR, ^{13}C NMR and IR spectra of the ligand 1,3-bis(salicylideneamino) propane and how the peaks will shift when it binds to the metal complex.

3 THE VSEPR THEORY

Valence shell electron pair repulsion (VSEPR) theory (1957) is a model in chemistry, which is used for predicting the shapes of individual molecules, based upon their extent of electron-pair electrostatic repulsion, determined using steric numbers. The theory is also called the Gillespie-Nyholm theory after the two main developers. The premise of VSEPR is that a constructed Lewis structure is expanded to show all lone pairs of electrons alongside protruding and projecting bonds, for predicting the geometric shape and lone-pair behaviour of a compound through consideration of the total coordination number.

VSEPR theory is based on the idea that the geometry of a molecule or polyatomic ion is determined primarily by repulsion among the pairs of electrons associated with a central atom. The pairs of electrons may be bonding or nonbonding (also called lone pairs). Only valence electrons of the central atom influence the molecular shape in a meaningful way.

3.1 Basic Assumptions

1. Pairs of electrons in the valence shell of a central atom repel each other.

2. These pairs of electrons tend to occupy positions in space that minimize repulsions and maximize the distance of separation between them.

3. The valence shell is taken as a sphere with electron pairs localizing on the spherical surface at maximum distance from one another.

4. A multiple bond is treated as if it is a single electron pair and the two or three electron pairs of a multiple bond are treated as a single super pair.

5. Where two or more resonance structures can depict a molecule the VSEPR model is applicable to any such structure.

Three types of repulsion take place between the pairs of electrons in a molecule:

- The lone pair-lone pair repulsion
- The lone pair-bonding pair repulsion
- The bonding pair-bonding pair repulsion.

A molecule must avoid these repulsions to remain stable. When repulsion cannot be avoided, the weaker repulsion (i.e. the one that causes the smallest deviation from the ideal shape) is preferred.

The lone pair-lone pair (lp-lp) repulsion is considered to be stronger than the lone pair-bonding pair (lp-bp) repulsion, which in turn is stronger than the bonding pair-bonding pair

(bp-bp) repulsion. Hence, the weaker bp-bp repulsion is preferred over the lp-lp or lp-bp repulsion.

VSEPR theory is usually compared (but not part of) and contrasted with valence bond theory, which addresses molecular shape through orbitals that are energetically accessible for bonding. Valence bond theory concerns itself with the formation of sigma and pi bonds. Molecular orbital theory is another model for understanding how atoms and electrons are assembled into molecules and polyatomic ions.

VSEPR theory has long been criticised for not being quantitative, and therefore limited to the generation of "crude", even though structurally accurate, molecular geometries of covalent molecules. However, molecular mechanics force fields based on VSEPR have also been developed.

3.2 AXE Method

The "AXE method" of electron counting is commonly used when applying the VSEPR theory. The A represents the central atom and always has an implied subscript one. The X represents how many sigma bonds are formed between the central atoms and outside atoms. Multiple covalent bonds (double, triple, etc) count as one X. The E represents the number of lone electron pairs present outside of the central atom. The sum of X and E, sometimes known as the steric number, is also associated with the total number of hybridised orbitals used by valence bond theory.

When the substituent (X) atoms are not all the same, the geometry is still approximately valid, but the bond angles may be slightly different than the ones where all the outside atoms are the same. For example, the double-bond carbons in alkenes like C_2H_4 are AX_3E_0, but the bond angles are not all exactly 120^0. Similarly, $SOCl_2$ is AX_3E_1, but because the X substituents are not identical, the XAX angles are not all equal.

3.3 Examples

Methane molecule (CH_4) is tetrahedral because there are four pairs of electrons. The four hydrogen atoms are positioned at the vertices of a tetrahedron, and the bond angle is $\cos^{-1}(-1/3)^0$ $109^o28'$. This is referred to as an AX_4 type of molecule. As mentioned above, A represents the central atom and X represents all of the outer atoms. Ammonia molecule (NH_3) has three pairs of electrons involved in bonding, but there is a lone pair of electrons on the nitrogen atom. It is not bonded with another atom; however, it influences the overall shape through repulsions. As in methane above, there are four regions of electron density. Therefore, the

overall orientation of the regions of electron density is tetrahedral. On the other hand, there are only three outer atoms.

Steric No.	Basic Geometry 0 lone pair	1 lone pair	2 lone pairs	3 lone pairs
1	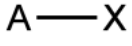 linear			
2	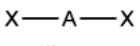 linear	Linear		
3	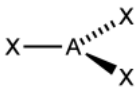 trigonal planar	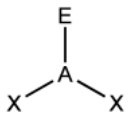 bent	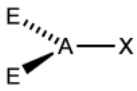 Trigonal Planar	
4	tetrahedral	trigonal pyramid	bent	linear
5	trigonal bipyramid	seesaw (chemistry)	T-shaped (chemistry)	linear
6	octahedral	square pyramid	square planar	
7	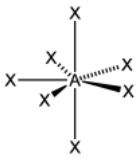 Pentagonal bipyramid	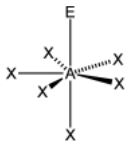 pentagonal pyramid		

Figure 3.1: Steric numbers and basic geometries.

Type	Shape	Geometry†	Geometry‡	Examples
AX_1E_*	Diatomic			HF, O_2
AX_2E_0	Linear			$BeCl_2$, $HgCl_2$, CO_2
AX_2E_1	Bent	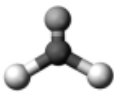	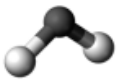	NO_2^-, SO_2, O_3
AX_2E_2	Bent		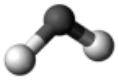	H_2O, OF_2
AX_2E_3	Linear			XeF_2, I_3^-
AX_3E_0	Trigonal planar	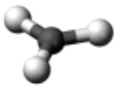	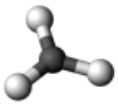	BF_3, CO_3^{2-}, NO_3^-, SO_3
AX_3E_1	Trigonal pyramidal		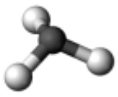	NH_3, PCl_3
AX_3E_2	T-shaped		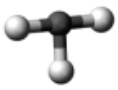	ClF_3, BrF_3
AX_4E_0	Tetrahedral	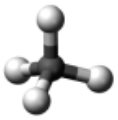	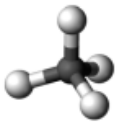	CH_4, PO_4^{3-}, SO_4^{2-}, ClO_4^-
AX_4E_1	Seesaw			SF_4
AX_4E_2	Square Planar		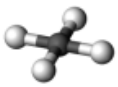	XeF_4
AX_5E_0	Trigonal Bipyramidal	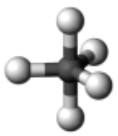	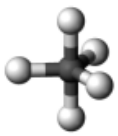	PCl_5
AX_5E_1	Square Pyramidal		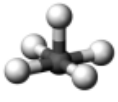	ClF_5, BrF_5
AX_6E_0	Octahedral			SF_6
AX_6E_1	Pentagonal pyramidal		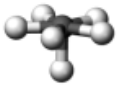	XeF_6

Figure 3.2: The AXE representation of some molecules and their respective geometries.

This is referred to as an AX_3E type molecule because the lone pair is represented by an E. The overall shape of the molecule is a trigonal pyramid because the lone pair is not "visible." The shape of a molecule is found from the relationship of the atoms even though it can be influenced by lone pairs of electrons.

A steric number of seven is possible, but it occurs in uncommon compounds such as iodine heptafluoride. The base geometry for this is pentagonal bipyramidal.

3.4 Symmetry Elements and Operations

3.4.1 Introduction

Symmetry provides us with a formal method for the description of the geometry of objects by describing the patterns in their structure. In chemistry, it is a powerful method that underlies many apparently disparate phenomena. Symmetry allows us to describe accurately the types of bonding that can occur between atoms or groups of atoms in molecules. It also governs the transitions that may occur between energy levels in molecular systems, which in turn allows us to predict the absorption properties of molecules and, hence, their spectra.

3.4.2 Symmetry Elements and Operations

3.4.2.1 Identity Operation, E

The identity operation is the simplest of all -- do nothing! It may seem pointless to have a symmetry operation that consists of doing nothing, but it is very important. All objects (and therefore all molecules) at the very least have the identity element. There are many molecules that have no other symmetry. For example CHFClBr contain no symmetry other than identity.

3.4.2.2 Proper Rotations: Cn

The geometric properties of shapes that make them symmetric can be classified by their symmetry elements. The validity of a symmetry element can be checked by carrying out the corresponding operation and then comparing the object with the starting point. For example, imagine constructing an axis for a water molecule which runs through the oxygen atom, bisecting the H-O-H angle, with the axis in the plane of the molecule. This construction is shown in Figure 1, which also illustrates the result of rotating the molecule by 180^o around the axis. After the rotation, we end up with a view of the water molecule identical to the starting point, so much so that if we had not labelled the hydrogen atoms it would be indistinguishable from the original. This result shows that the axis we have drawn is a symmetry element of the molecule and the act of rotating the molecule is the corresponding symmetry operation. The rotation operation also shows that the two hydrogen atoms in the water molecule are equivalent; if a symmetry operation can interchange two atoms, then the atoms must occupy

identical chemical environments.

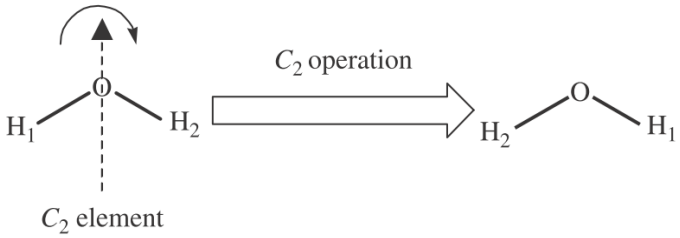

Figure 3.3: The C_2 symmetry element of water and the result of the C_2 operation.

Rotational elements and operations are labelled using a capital C. For rotations by 180° there are two positions of the molecule which appear identical, the starting point and the molecule after the rotation, so a subscript 2 is added to the label: C_2. This subscript is known as the order of the rotation axis.

To emphasise the difference between elements and operations further, consider the structure of ammonia shown in Figure 2. A C_3 axis is present: the symmetry element is a line running through the nitrogen atom and the centre of the triangle formed by the three hydrogen atoms.

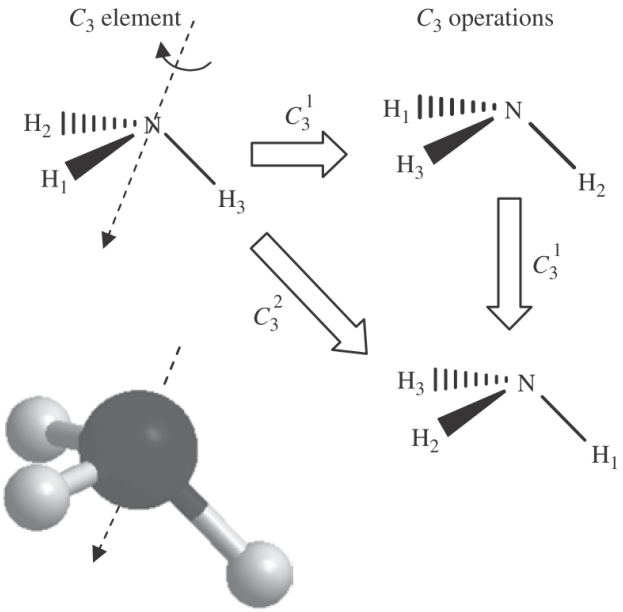

Figure 3.4: The C_3 axis of ammonia and the corresponding operations.

The C_3 axis actually has two symmetry operations associated with it, as can be seen in Figure 2: a rotation by 120° and a rotation by 240°. By convention, a rotation operation moves the atoms clockwise when looking down the axis direction. In the first step of the operation sequence shown in Figure 2, a clockwise rotation by 120° takes each hydrogen atom to the position of one of its neighbours. A second application of the operation takes each hydrogen

atom to the original position of its other neighbour. To distinguish the two operations we add a superscript to indicate how many times the operation has been applied. So C_3^2 means that, starting from the original configuration, two successive rotations of 120° are applied, i.e. a total of 240°.

Molecules may contain more than one rotation axis, and those axes may have different orders. In this situation, the highest order axis is termed the principal axis. As an example, Figure 3 shows the structure of ferrocene (dicyclopentadienyliron(II)). This complex has a C_5 axis, which is the line joining the centres of the cyclopentadiene rings through the Fe centre (Figure 3a). In addition, there are five C_2 axes that run through the Fe atom parallel to the ring systems and perpendicular to the principal axis. These are best seen looking down the principal axis direction, as shown in Figure 3b. The C_2 rotation operations cause the exchange of the cyclopentadiene rings, whereas the C_5 operation simply rotates each cyclopentadiene ring around its centre. There is a convention that molecules are orientated so that the principal axis defines the vertical direction and that this is also aligned with the Cartesian Z-axis. This means that the vertical direction in Figure 3a runs up the page, whereas 'vertical' in Figure 3b is into the page.

The symmetry elements for a molecule are fixed in space: as we move the atoms under a given operation the symmetry elements are not shifted. For ferrocene, the atoms of the complex can be moved between any of five arrangements using the principal axis. In any of these, each of the C_2 axes remains a symmetry element.

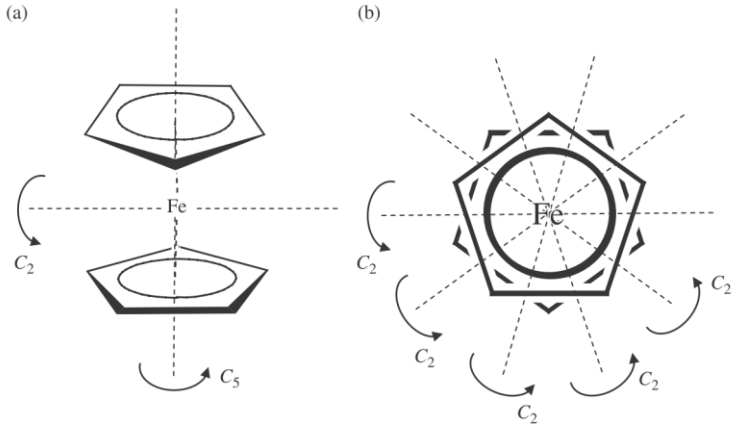

Figure 3.5: The structure of ferrocene, illustrating (a) the C_5 axis and an example C_2 axis;(b) a plan view of the molecule showing all five C_2 axes.

A further possibility for multiple rotation axes is to have more than one candidate for the principal axis. For example, the highest order axis for ethene is a twofold axis, but there are three nonequivalent C_2 axes, as shown in Figure 4. The choice of principal axis is now arbitrary, and it is usual to assign each axis a Cartesian label (X,Y or Z) so that they can be

referred to explicitly.

3.4.2.3 The Plane of Symmetry: σ

If a plane exists for which reflection of each atom in a molecule gives an indistinguishable configuration, the molecule is said to have a plane of symmetry, which is given the label σ.

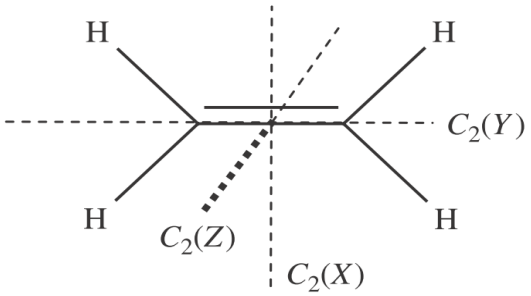

Figure 3.6: The structure of ethene showing three distinct C_2 axes.

The symmetry element is the plane itself, since all points in the plane remain unchanged by the operation of reflection. For the water molecule there are two planes of symmetry, as shown in Figure 5. These are distinguished by labelling the plane perpendicular to the molecule σ and the plane of the molecule itself σ'. The C_2 axis of water is the only axis, and so it is also the principal axis defining the vertical direction. This means that the mirror planes are standing vertically, and so a subscript is added to remind us of this, giving σ_v and $\sigma_{v'}$.

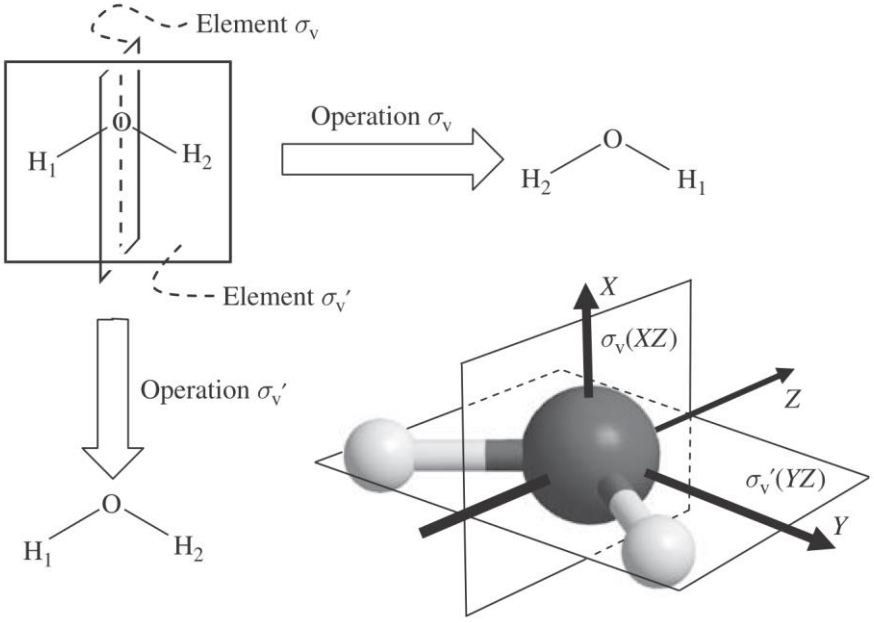

Figure 3.7: The two mirror planes for the H_2O molecule showing the difference between σv and σvιoperations. The inset shows the relationship between the mirror planes and a reference axis system.

Which plane is which is a somewhat arbitrary choice; however, the designation described here is quite widely used and is based on the alignment of the symmetry planes with the Cartesian axis system. Figure 3.7 shows that the two planes intersect in the line of the C_2 axis we identified earlier; the planes of symmetry are said to contain the rotational axis. The principal axis gives us the Cartesian Z-direction, which, in this case, is in the molecular plane. We also take Y to be in the molecular plane, and so X must be perpendicular to it. The full labels for the mirror planes of water become σ_v (XZ) and $\sigma_{v'}$ (YZ), but it is common to omit the Cartesian parts of these labels.

Some molecules have multiple axes and mirror planes. For example, boron trifluoride (BF_3) is a planar molecule with a C_3 axis perpendicular to the plane and passing through the boron atom, as shown in Figure 3.8. However, there are also C_2 axes in the plane of the molecule which run along each of the B-F bonds.

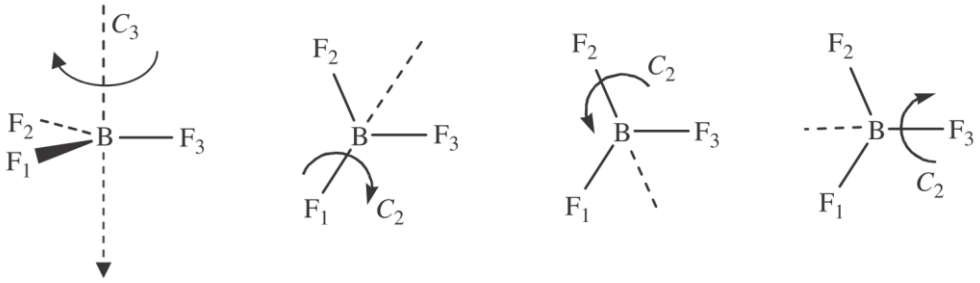

Figure 3.8: The rotational symmetry elements of BF_3.

The highest order axis present is taken to be the principal axis and gives us the 'vertical' direction. So, BF_3 has three vertical mirror planes, each of which contains a B-F bond; an example of a vertical mirror plane in BF_3 is shown in Figure 7a. The C_3 operations will move the fluorine atoms between these planes, but each will always contain one fluorine atom and reflect the other two into one another. So, although there are three vertical planes, they are identical, requiring only the single label σ_v, and there are three σ_v operations. The plane of the molecule for BF_3 is also a plane of symmetry, as illustrated in Figure 3.9b. This contains all three of the B-F bonds, but not the principal axis. In fact, the plane is perpendicular to the C_3 axis, i.e., the plane is horizontal and so is labelled σ_h.

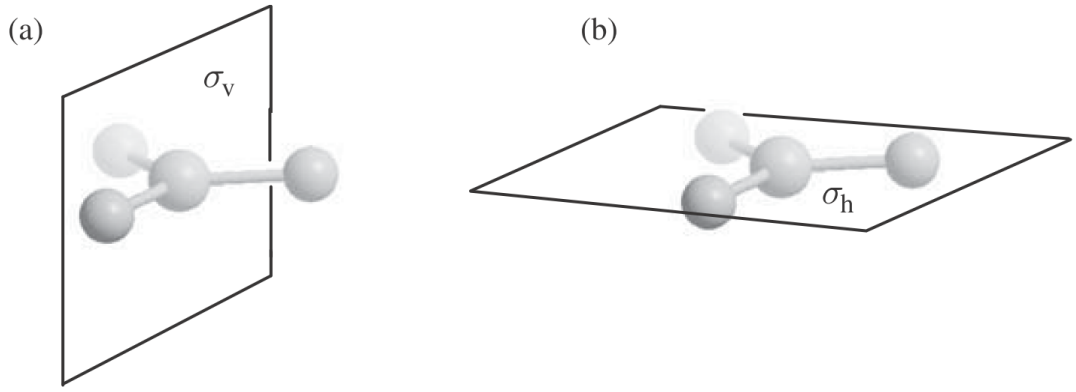

Figure 3.9: The two types of symmetry plane for BF_3 : (a) an example of a vertical plane; (b) the horizontal plane σ_h .

3.4.2.4 The Inversion Centre: i

So far, we have looked at symmetry operations for which the corresponding elements are the plane (a reflection operation) and a line (the rotation operation). The next symmetry element is the inversion centre, labelled i. The operation of inversion leaves only a single point unchanged, and so it is often referred to as a centre, or point, of symmetry. The inversion operation is illustrated in Figure 3.10 with two pairs of points, A, A' and B, B', which represent atoms in a hypothetical molecule. For each pair, the points are equidistant from the inversion centre, and the lines between A - A' and between B - B' include i. To perform the inversion operation we imagine moving each atom in the molecule along a straight line to the inversion centre and then moving them along the same line beyond the centre to a distance equivalent to their starting point. For the hypothetical example, A and A' would be interchanged, as would B and B'. If the inversion operation result is indistinguishable from the initial geometry, then the molecule has an inversion centre. The inversion operation can be thought of as similar to the reflection operation, but referred to a point rather than a plane.

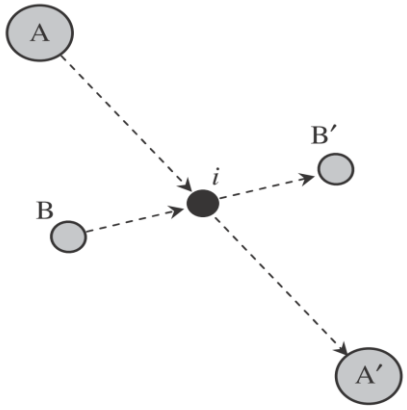

Figure 3.10: An illustration of the inversion centre operation. Under inversion, each point in a molecule is moved through the inversion centre to a position on the opposite side of the centre and at the same distance from the centre as the original point. In this case, atom pairs

A A′ and B′ are linked by the inversion centre i.

Square planar species, such as the $[PtCl_4]^{2-}$ ion shown in Figure 9a, has a centre of inversion. On inversion, the chlorine atoms *trans* to each other in the original molecule are interchanged.

However, in three dimensions the inversion operation will swap left with right, top with bottom and back with front simultaneously. For this to be a symmetry operation which leaves the molecule unchanged, the centre of inversion symmetry element will always be at the centre of the structure. So the Pt atom in $[PtCl_4]^{2-}$ remains in the same position after the operation. Figure 3.11b shows the three-dimensional example SF_6 ; here, the central S atom is on the inversion centre and so remains in the same place after inversion, but, with the F atoms labelled, it can be seen that atoms trans to one another are again swapped over. The molecular models of these two structures in Figure 3.11c should help to visualise the process.

3.4.2.5 Improper Rotation: S_n

The Improper Rotation element involves a 360/n degree rotation, followed by a reflection through a mirror plane (σ) perpendicular to the rotation axis. The molecule that results from this rotation-reflection is indistinguishable from the original. Thus the S_n symmetry element is composed of a $C_{n/2}$ followed by a σ. However, a molecule with an S_n element might contain neither a C_n nor a σ (although it will have $C_{n/2}$'s coincident with the S_n's). Molecules which contain an improper axis of rotation are achiral. An S_1 is equivalent to a mirror plane, and an S_2 is equivalent to an inversion centre; these operations prohibit chirality.

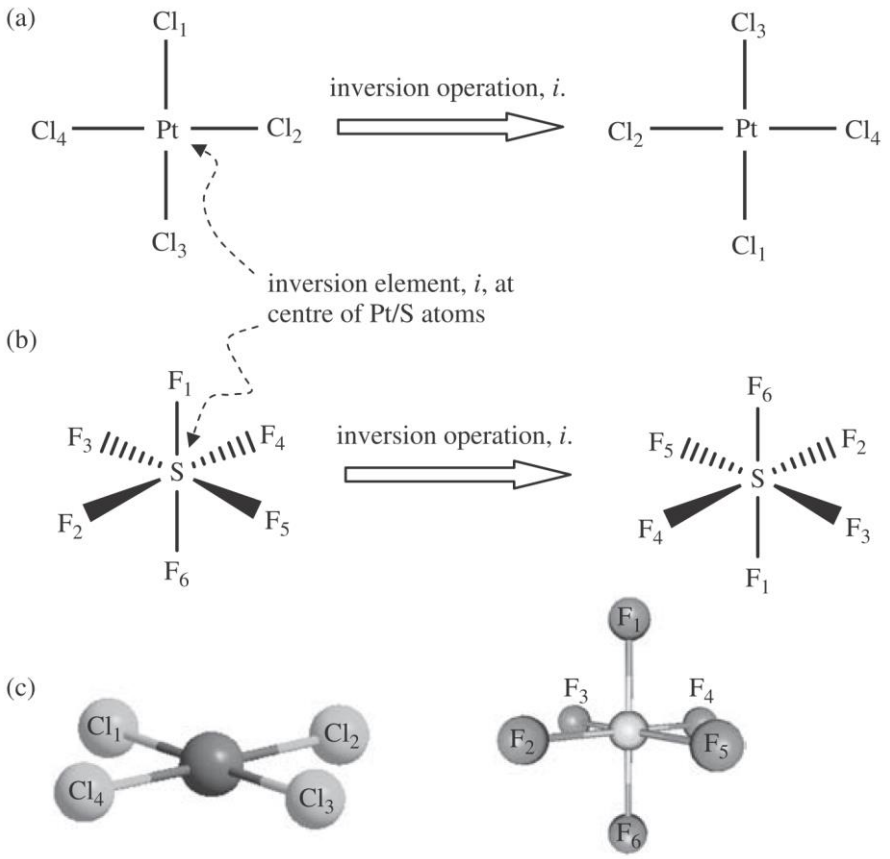

Figure 3.11: The inversion element and operation for (a) a chemical complex $[PtCl_4]^{2-}$ and (b) the molecule SF_6 . (c) Ball and stick representations of the two structures used in (a) and (b).

Methane, CH_4, contains the S_4 symmetry element. Rotation of 90° about the axis, followed by a reflection through a mirror plane perpendicular to that axis gives a molecule indistinguishable from the original. Note that methane does not have a C_4 rotation axis (although it does have C_2's coincident with the S_4's). While methane does have mirror planes, none are perpendicular to the S_4 element.

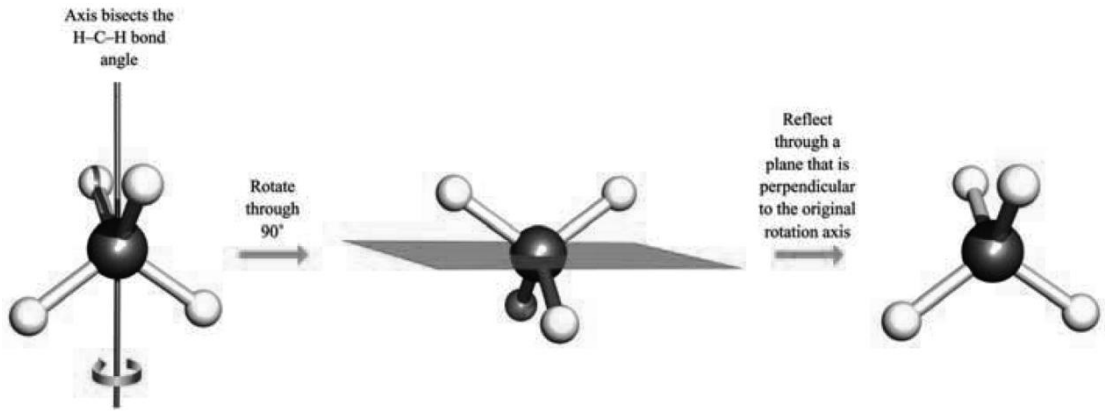
Axis bisects the H–C–H bond angle
Rotate through 90°
Reflect through a plane that is perpendicular to the original rotation axis

Figure 3.12: Note: Neither C_4 nor the $\sigma_\perp$ is a symmetry operator of methane but their product $C_4 \times \sigma_\perp$ is S_4.

3.4.3 POINT GROUPS

Whether or not a molecule has all or some of these symmetry elements can easily be classified by assigning a label. This label identifies the point group of the molecule. There are many, many point groups possible, but only a few are common for molecular structures.

Some of the most common points that you will be seeing include:

C_{2v} (which describes water, H_2O)

C_{3v} (which describes ammonia, NH_3)

T_d (tetrahedral, which describes methane CH_4)

D_{2h} (which describes ethylene, H_2CCH_2)

O_h (octahedral, which describes sulphur hexafluoride, SF_6)

Assigning a point group to a molecule depends on listing the symmetry elements of the molecule and then looking them up in point group decision tree.

3.4.4 Examples of the Impact of Geometric Symmetry on Chemistry

The use of symmetry to identify equivalent atoms or groups in molecules already allows some insight to be gained into the way symmetry can be used to interpret the chemical behaviour of molecules possessing, or lacking, the symmetry elements introduced so far. We can also start to explore how symmetry helps deduce chemical structure from experimental data.

3.4.4.1 Oxygen Transfer via Metal Porphyrins

Rotation axes and mirror planes are very common symmetry elements in molecules and can lend important properties to the structure. For example, in biology, the porphyrin ring (Figure 3.13) is the basic structure of an important class of tetradentate ligands. The idealized unsubstituted ring has a C_4 principal axis at its centre perpendicular to the plane of the ring. This will give rise to two C_4 (C_4 and C_4^3) and one C_2 (C_4^2) operations. Figure 3.13 also shows that there are four C_2 axes in the plane of the ring: two $C_{2'}$ and two $C_{2''}$. Each of these axes can be used to turn the planar molecule over so that the upper and lower faces are interchanged. Since this is achieved through symmetry operations, it implies that the two faces of the ring are identical. This does have important consequences for the biological processes involving porphyrin rings. In particular, complexes of Fe^{2+} with more elaborate porphyrin ligands are essential for the function of haem, which is involved in oxygen storage in the haemoglobin component of blood. When it is oxygenated, the central Fe atom carries a single oxygen atom which sits above the plane of the ring and it is coordinated by part of the host protein structure from below. Since the two faces of the porphyrin ligand are linked by symmetry operations, it does not matter ‘which way up’ the porphyrin is orientated as it is incorporated into the protein.

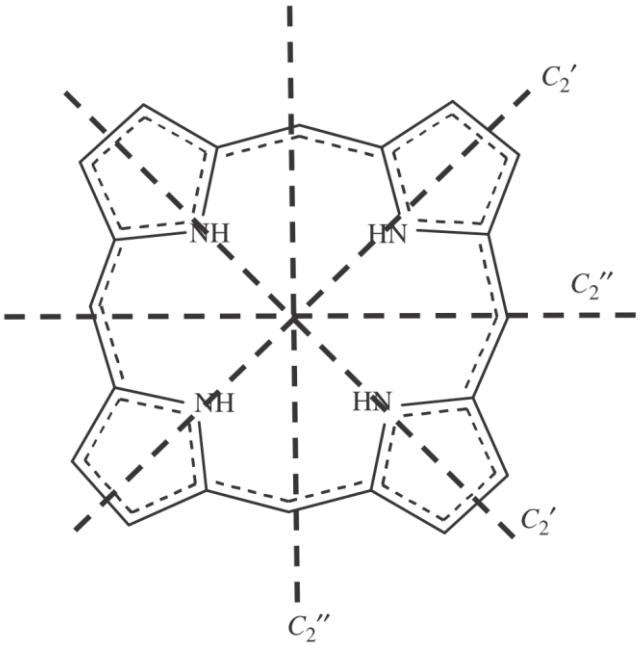

Figure 3.13: The porphyrin ring structure. A C_4 axis passes through the centre of the ligand perpendicular to the molecular plane. The four C_2 axes shown in the molecular plane form two sets of two, labelled $C_2$and $C_{2''}$.

3.4.5 Infrared Spectroscopy

The IR spectrum of benzene is very simple, showing only four main bands. On substitution with a single fluorine atom to give fluorobenzene, the spectrum becomes much more complex, with many more bands appearing between 400 and 1600 cm^{-1}. We know that IR spectra are the result of radiation exciting vibrational modes in a molecule. The number of possible lines is related to the number of vibrational modes for the molecule in question. Since each atom in a molecule can move in three dimensions (X, Y, Z), both benzene and fluorobenzene will have a total of 36 degrees of freedom. For a nonlinear molecule there are six degrees of freedom associated with the motion of the molecule as a whole (three translations and three rotations), and these are not vibrations. So, we expect the number of vibrational modes for a molecule containing N atoms to be 3N−6. Both benzene and fluorobenzene have 12 atoms, and so have 30 vibrational modes. The fact that this does not result in 30 IR absorptions is a result of the symmetry of the molecules; and because benzene is 'more' symmetric than fluorobenzene, fewer modes of vibration are detected in the spectrum of benzene than in that of fluorobenzene.

To understand and quantify these differences in spectra we need more rigorous definitions of symmetry than simply saying benzene is 'more' symmetric than fluorobenzene. The geometric constructs of molecular symmetry help us to define a molecule's symmetry and the use of group theory allows us to predict the number of absorption lines that will be observed.

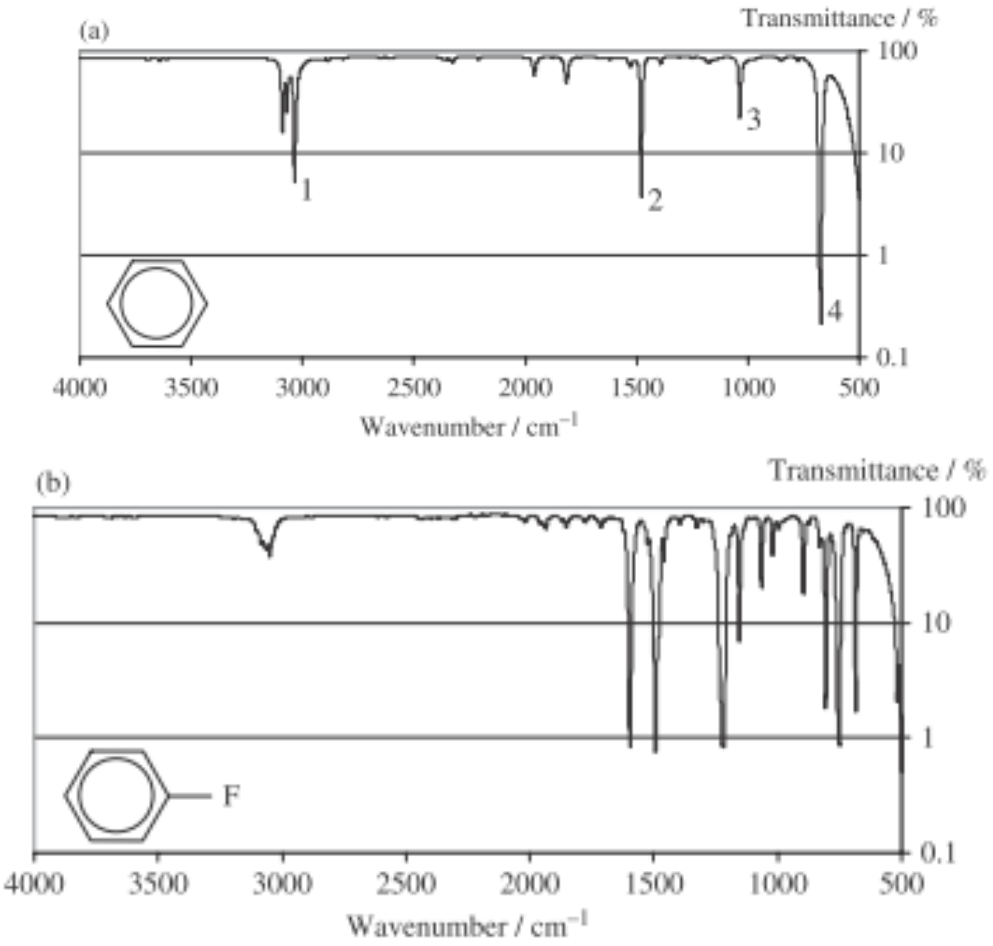

Figure 3.14: The infrared spectra of (a) benzene and (b) fluorobenzene.

3.4.6 Nuclear Magnetic Resonance: Chemical Equivalence

The chemical shifts from a ^{1}H NMR spectrum are used as an indication of the chemical environment of each proton in the molecule of the sample. If two hydrogen atoms are linked by a symmetry operation, then they will have the same environment and are referred to as chemically equivalent. The line in the ^{1}H NMR spectrum for each will occur at exactly the same position, and so the intensity of the peak at this chemical shift will be twice that of a hydrogen atom in a unique environment, i.e. not linked to any other hydrogen atoms by symmetry operations. This allows us to use the intensity of the peaks as an indication of the number of equivalent hydrogen atoms in a molecule and so may help to determine the sample's molecular structure.

As an example, Figure 3.16 shows a computer-generated ^{1}H NMR spectrum for a compound with the chemical formula C_8H_{14}. There are several possibilities for the molecular structure of this sample, two of which are given in Figure 3.17. The spectrum shows two peaks with the lower chemical shift having a height six times that of the other signal.

Only bicyclo[2.2.2]octane has a structure consistent with the spectrum, since the two hydrogen atoms that lie on the principal axis (C_3) are linked by σ_h and by i and all of the other

12 hydrogen atoms are linked by combinations of σ_h , σ_v , C_3 and i operations. None of the symmetry operations would interchange the axial hydrogen atoms with any of the hydrogen atoms in the CH_2 groups, and so there are two distinct sets of hydrogen atoms. This gives the same division of the hydrogen atoms between the two environments that was implied from the spectral data. The dimethylcyclohexene alternative has only a C_2 axis and no other symmetry axes or planes. As we shall see below, this means that it has hydrogen atoms in at least three different environments, and so would be expected to give a more complex ^{1}H NMR spectrum.

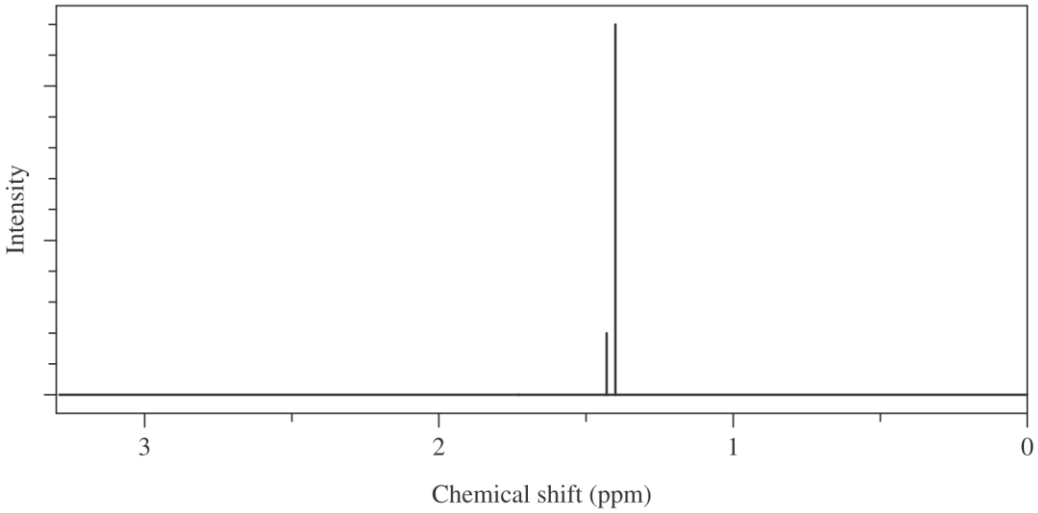

Figure 3.15: ^{1}H NMR spectrum for a compound with the chemical formula C_8H_{14} .

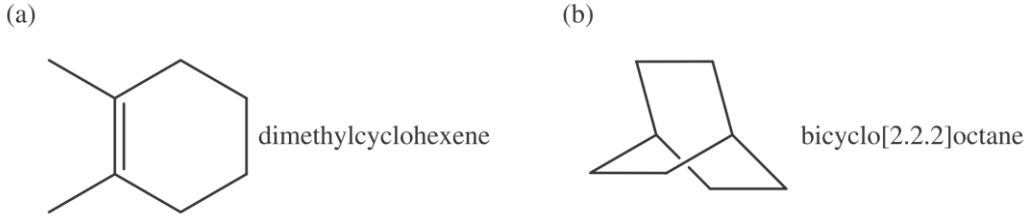

Figure 3.16: Two possible molecular structures for the chemical formula C_8H_{14}.

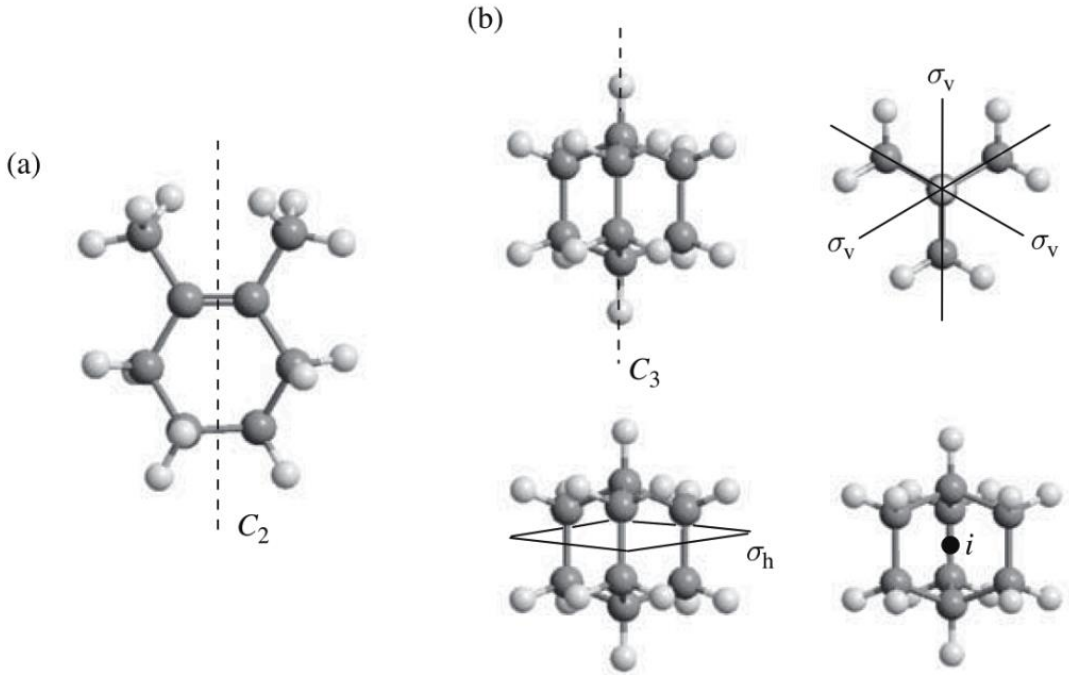

Figure 3.17: (a) The C2 axis in dimethylcyclohexene and (b) the principal C3 axis and example symmetry planes for bicyclo[2.2.2]octane.

Point Group Designations

Point Group	Example
C_1: E. No symmetry elements are present.	C_1
C_s: E, σ. Molecule has a mirror plane of symmetry	C_s
C_i: E, i. Molecule has an inversion center	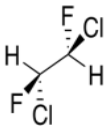 C_i
S_n: E, S_n. In many cases there will also be a $C_{n/2}$ rotation axis, although this is not a requirement. Note that S_1 is the same as a mirror plane (σ) and should be called C_s. S_2 is the same as i and should be called C_i.	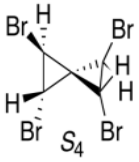 S_4
C_n: E, C_n. Molecule has only a single rotation axis, with no mirror planes.	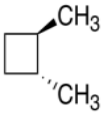 C_2
C_{nv}: E, C_n, and n σ_v. Molecule vertical mirror planes corresponding to the C_n rotation.	C_{3v}
$C_{\infty v}$: linear unsymmetric molecule. A special case of C_{nv}.	O=C=S $C_{\infty v}$
D_n: E, C_n, and n C_2 axes ⊥ to C_n axis: Thus a D_3 molecule would have 3 C_2 ⊥ to the C_n axis.	D_2
D_{nh}: E, C_n, n C_2 axes, σ_h. In addition to the n C_2 axes there is a horizontal mirror plane.	D_{6h}
$D_{\infty h}$: Special case of D_{nh} for linear symmetric molecules.	O=C=O $D_{\infty h}$
D_{nd}: E, C_n, n C_2 axes, and n σ_v (also known as σ_d).	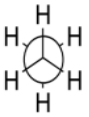 D_{3d}

Figure 3.18: Point group designations.

POINT GROUP DECISION TREE

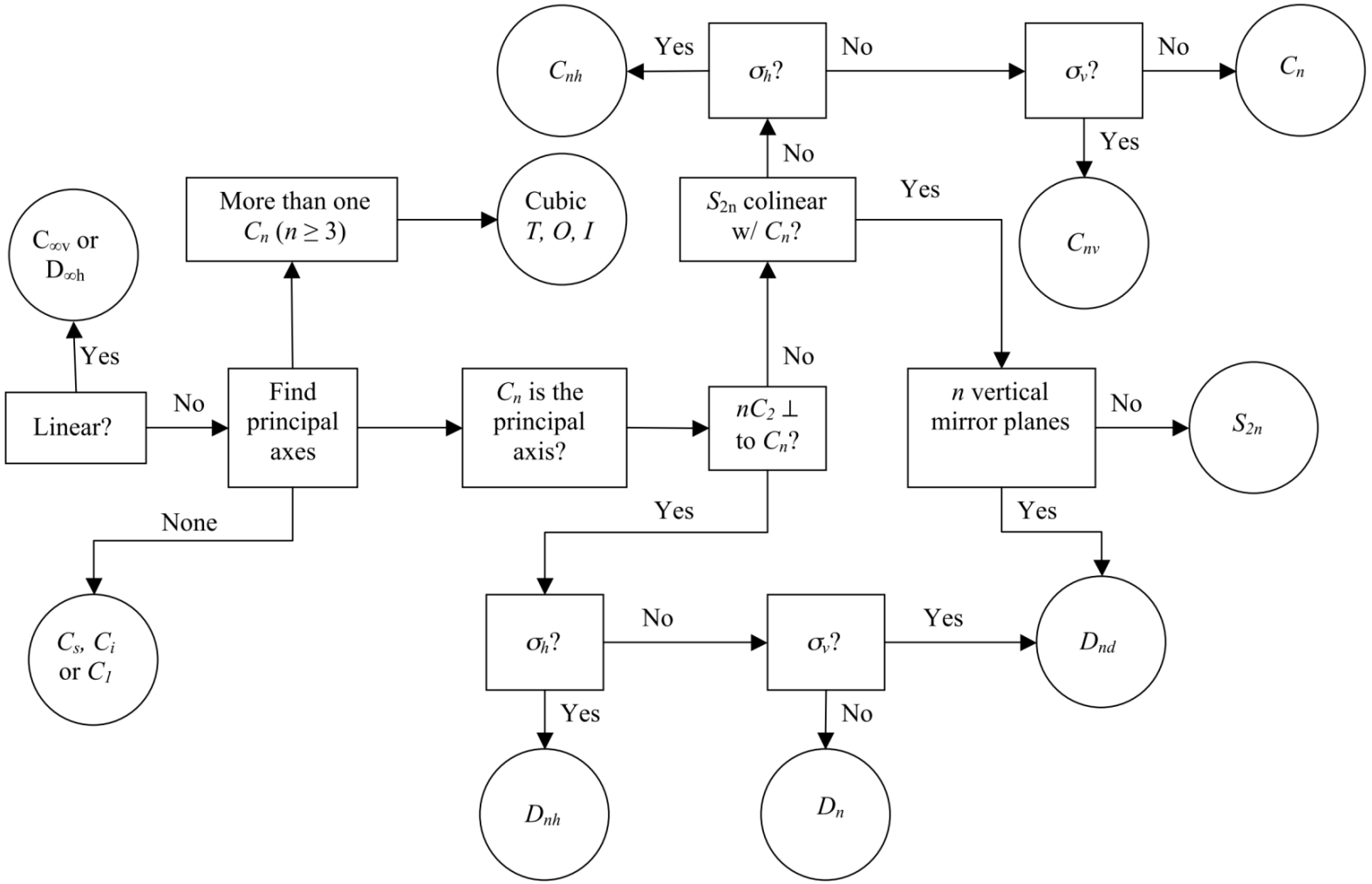

3.4.7 Self-Test Questions

1. For each of the molecules in Figure 3.19 identify all of the rotation axes present, giving the order of each axis. You should make sketches of the molecules viewed from different directions to illustrate your answer.

2. Identify all the mirror planes present in the molecules of Figure 3.19 and use the rotation axes you have found to label them as σ_v , o_r σ_h.

3. Identify point groups for each of the molecules in Figure 3.19.

4. How many distinct ^{1}H NMR peaks would you expect for each molecule containing H atoms in Figure 3.19?

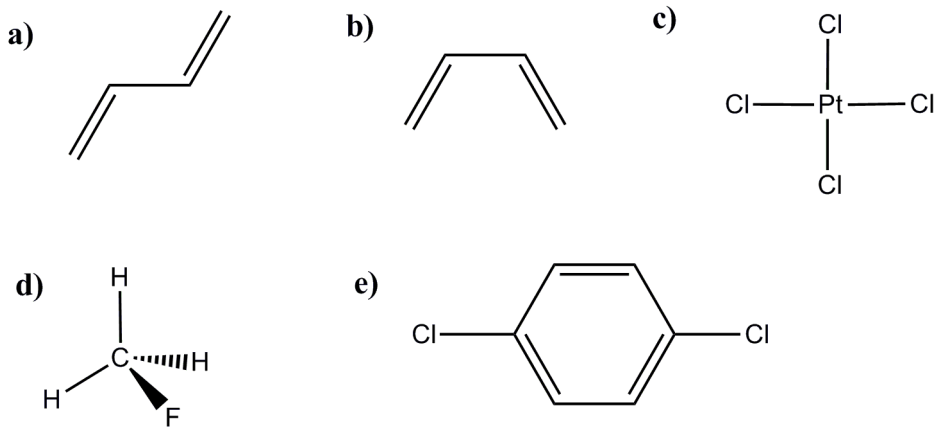

Figure 3.19: Example molecules for symmetry analysis.

3.5 References

1. Molecular Symmetry, David J. Willock, 2009 John Wiley & Sons, Ltd. ISBN: 978-0-470-85347-4

2. http://www.saylor.org/site/wp-content/uploads/2011/06/VSEPR-Theory.pdf

4 POTASSIUM BIS(OXALATO)CUPRATE(II) DIHYDRATE: PREPARATION AND ANALYSIS

4.1 Theory

The high natural abundance and high concentrations of copper and copper ores make copper an economical choice for many industrial applications. Copper may exist in three oxidation states, +1, +2, and +3. However, most copper compounds are commonly encountered as salts of Cu^{2+}, while Cu^{3+} is the least stable form. Copper, being a transition metal, also forms coordination compounds.

In this experiment, potassium bis(oxalato)cuprate(II) dihydrate will be prepared by reaction of copper(II) sulfate pentahydrate with potassium oxalate:

$$CuSO_4.5H_2O_{(aq)} + 2\ K_2C_2O_{4(aq)} \rightarrow K_2Cu(C_2O_4)_2.2H_2O_{(s)} + K_2SO_{4(aq)} + 3H_2O_{(l)}$$

The number of oxalato ligands in the complex ion will be determined by titration with standard permanganate solution. The copper content of the complex ion will be determined by iodine-thiosulfate titration.

4.2 Chemicals

Copper(II) sulfate pentahydrate, $CuSO_4.5H_2O$
Potassium oxalate monohydrate, $K_2C_2O_4.H_2O$
Sulfuric acid, $H_2SO_{4\ (aq)}$
Potassium permanganate, $KMnO_4$
Sodium carbonate, Na_2CO_3
Potassium iodide, KI
Sodium thiosulfate, $NaS_2O_{3\ (aq)}$
Starch indicator (freshly prepared, 5% w/v)
Potassium thiocyanate, KSCN

4.3 Glassware

- Erlenmeyer flasks, 250 mL
- Beakers, 50 mL
- Funnel
- Pipettes, 5 mL, 10 mL
- Burettes (2)
- Graduated cylinder, 50 mL

- Stirring rod
- Filter paper
- Heater-stirrer apparatus.

4.4 Preparation of potassium bis(oxalato)cuprate(II) dihydrate

a. Dissolve 6 g of $CuSO_4.5H_2O$ in 15 mL of hot water and heat the solution to 90°C.

b. Dissolve 17.6 g of potassium oxalate monohydrate in 100 mL hot water and heat the solution to 90°C.

c. Slowly add the copper(II) solution to the oxalate solution with stirring. (If you reverse the order of mixing the crystals formed are usually found to be smaller).

d. Cool the mixture in ice water and filter off the blue crystals. Wash with 2 x 5 ml portions of ice-cold water and 10 mLof ethanol (NO FLAMES !!).

e. Air dry the product and determine the yield.

4.5 Determination of the oxalate content

Weigh accurately about 0.20-0.25 g of your product into an erlenmeyer flask and dissolve the complex by adding about 25 mL of water. Add 20 mL of 2.5 M sulphuric acid and heat the solution to about 80°C.

$$H_2SO_{4\,(aq)} + K_2Cu(C_2O_4)_2.2H_2O_{\,(s)(aq)} \rightarrow K_2C_2O_{4\,(aq)} + CuSO_{4\,(aq)} + H_2C_2O_{4\,(aq)} + 2H_2O_{\,(l)}$$

Titrate the solution with standardised 0.02 M potassium permanganate solution, until the colour of the solution becomes pink persistent for 1-2 minutes (end-point). Note that during the initial stages of the titration the solution is cloudy due to undissolved complex. This should have a clear appearance during the titration. The temperature should not be less than 60° C at the end point. If it falls below this during the titration, the solution must be reheated. Record the volume of standard $KMnO_4$ solution used. Take care not to go beyond the endpoint as the presence of a large excess of permanganate makes the copper determination difficult. You should repeat the titration twice. The results of the two analyses should be consistent. Otherwise a third determination should be done. Compare your results with the theoretical value.

$$16H^+_{(aq)} + 2MnO_4^-{}_{(aq)} + 5C_2O_4^{2-}{}_{(aq)} \rightarrow 10CO_{2(g)} + 2Mn^{2+}_{(aq)} + 8H_2O_{(l)}$$

4.6 Determination of the copper content

Ensure that the solution obtained above contains no excess permanganate by boiling until

the purple colour is discharged. Add solid Na_2CO_3 to the cooled solution until a precipitate first appears. Then add dilute acetic acid (10% w/v) until the pH is about 5. Finally, add about 1 g of solid potassium iodide into the solution.

$$Na_2CO_{3(aq)} + CuSO_{4(aq)} \rightarrow Na_2SO_{4(aq)} + CuCO_{3(s)}$$

$$2Cu^{2+}_{(aq)} + 5I^-_{(aq)} \rightarrow 2CuI_{(s)} + I_3^-{}_{(aq)}$$

Titrate the liberated iodine which forms the I_3^- ion with standardized 0.050 M sodium thiosulfate solution using freshly prepared 5% (w/v) starch solution as indicator. A sharper end-point is obtained by the addition of 1-2 g potassium thiocyanate as the end-point is approached.

$$I_3^-{}_{(aq)} + 2S_2O_3^{2-}{}_{(aq)} \rightarrow 3I^-_{(aq)} + S_4O_6^{2-}{}_{(aq)}$$

4.7 Determination of the hydrate content

Weigh the 1.5-2 g the hydrate in a crucible and heat it. Allow the crucible to cool to room temperature in a desiccator, and then weigh it again. Repeat the procedure up to constant weight. Determine the hydrate, from the difference of first and last weight.

4.8 Qualitative work

Prepare a solution of the product in distilled water and add a few drops of potassium iodide solution. Test for the presence of iodine by adding a little chloroform and shaking the tube. Acidify with dilute sulphuric acid and shake the tube.

Compare the above with the reaction of a dilute solution of copper sulfate. Account for the differences in terms of the structure of the complex ion.

4.9 Treatment of data

1. Calculate the % yield of potassium bis(oxalato)cuprate(II) dihydrate prepared.

2. Calculate the weight % of oxalate present in potassium bis(oxalato) cuprate(II) dihydrate complex. Compare the experimental value with the theoretical value.

3. Write the oxidation reduction reactions involved for the determination of copper content.

4. Calculate the weight % of copper present in potassium bis(oxalato) cuprate(II)dihydrate. Compare the experimental value with the theoretical value.

5. Calculate the weight % of hydrate present in potassium bis(oxalato) cuprate(II)dihydrate. Compare the experimental value with the theoretical value.

6. Discuss diamagnetic or paramagnetic of Cu complex.

7. Calculate the coefficient of the complex. Compare the experimental coefficient with the theoretical coefficient.

8. Calculate the required amounts of $KMnO_4$ and $Na_2S_2O_3$ that reacted.

4.10 References

Preparatory Problems 43rd International Chemistry Olympiad, Editor: Saim Özkar, Ankara.

J.D. Woollins, Inorganic Experiments, VCH, Weinheim, 1994.

5 PREPARATION AND INVESTIGATION OF SOME COORDINATION COMPOUNDS

5.1 Special Safety Precautions

1. Ammonia solutions are irritating to skin and eyes, and the vapour must not be inhaled. Wear rubber gloves and safety goggles when handling ammoniacal solutions and work in a fume cupboard. If ammonia is splashed on your skin, wash it off with plenty of water. Provided you do this immediately there is no cause for alarm.

2. Oxalic acid and oxalates are toxic and must not be ingested.

3. Hydrogen peroxide can cause burns, and skin contact must be avoided. Wear rubber gloves.

Note on the concentration of hydrogen peroxide: Bottles of hydrogen peroxide are traditionally labelled "20 vol", "100 vol", etc., meaning the following: litre of the solution, when decomposed according to the equation $2H_2O_2 \leftrightarrow 2H_2O + O_2$, yields 20 (etc.) litres of oxygen gas, at standard temperature and pressure. "20 volume" hydrogen peroxide contains ca. 6% H_2O_2 by weight.

If you are supplied with hydrogen peroxide labelled in this way, be sure to select the correct bottle. In your notebook, lake care to record the concentration in the form specified on the label. In your report, however, be sure to mention the molar concentration as well as the "vols".

5.2 Experimental

5.2.1 Instructions for Course Organisers

1. Do not use "100 vol" hydrogen peroxide; 10 or 20 vol is sufficient.
2. Laboratory Technical staff needs instructions to make saturated oxalic acid.
3. Supply references to the standard inorganic text book used in your course.

5.2.2 Hexaamminenickel(ll) tetrafluoroborate $[Ni(NH_3)_6](BF_4)_2$,

Dissolve about 3 g of hydrated nickel chloride, $NiCl_2.6H_2O$, in 5 mL of warm water, and filter, if necessary, to remove any insoluble matter. Then slowly add 5 to 6 mL of concentrated aqueous ammonia (specific gravity 0.88 g cm^{-3}) stirring until all the initial green precipitate of

nickel hydroxide has dissolved. The clear deep blue liquid now contains a copious crystalline deposit of the violet nickel hexaammine chloride. If this does not appear, leave it to stand for 5 minutes in a beaker of ice. If the solution is not clear blue add another 1 mL of 0.88 g cm^{-3} ammonia.

Redissolve the crystals by careful addition of a minimum (less than 8 mL) of cold water, added in 0.5 mL portions with continuous stirring. Take care not to hydrolyse the complex with excess water. Finally, filter off any small insoluble residue.

Dissolve approximately 2.5 g of ammonium tetrafluoroborate in dilute aqueous ammonia (ca. 2 mol dm^{-3}) and add this to the solution of the nickel ammine chloride. The sparingly soluble hexaammine nickel tetrafluoroborate is immediately formed as a crystalline precipitate. Filter by suction and wash the precipitate with aqueous ammonia until the filtrate (solution) is colourless. Finally, wash with acetone. Allow the mauve crystals to dry in a desiccator. Record the yield in your notebook.

5.2.3 Potassium Tris(oxalato)ferrate(III)

Dissolve 15 g of ammonium ferrous sulfate $(NH_4)_2Fe(SO_4)_2.6H_2O$ in 50 mL of hot water acidified with dilute sulphuric acid. Add a hot solution of 7.5 g of oxalic acid in 50 mL of water. Cautiously heat the mixture to boiling and then allow the yellow precipitate of iron(II) oxalate, $FeC_2O_4.2H_2O$, to settle. Cool the solution. Wash the precipitate with 30 mL of water by decantation. Repeat the washing two to three times.

Now add a warm solution of 10 g of potassium oxalate monohydrate $K_2C_2O_4.H_2O$ in 30 mL of water. Add slowly, with m teat pipette, 25 mL of '20 volume' hydrogen peroxide (see Special Safety Precautions), stirring the solution continuously and keeping the temperature below 40 ^oC. Any effervescence indicates that the solution is too hot. Then heat the mixture, which now contains some ferric hydroxide, to nearly boiling. The precipitate is now brown. Add a saturated solution of oxalic acid until the precipitate just dissolves again. Filter the solution whilst still hot and finally add 30 mL of methylated spirit, leave to crystallise in the dark.

When green crystals of the complex have appeared (probably the next day) filter the solution and wash the crystals in acetone. Allow them to dry at room temperature in the dark. Store the product in a glass specimen tube, wrapped in aluminium foil.

5.3 Chemical Properties

The object of the following tests is to give you experience in observing and identifying the products from reactions of transition metal complexes. Make notes in your laboratory notebook of your observations, as you make them. In your report, summarise your

observations and try to write equations and explanations for the reactions.

5.3.1 Thermal decomposition of hexaamminenickel(II) tetrafluoroborate

Heat 0.3 g of your product carefully in a large dry test tube and record your observations (colour changes, gas evolution, etc,}. Test both the residues and the sublimates for both boron and fluorine. Suitable tests can be found in Vogel's Qualitative Analysis. (6th ed. revised by G. Svehla. Longman Scientific). Note that any test which might involve the evolution of HF must be carried out on a small scale and in a fume cupboard. Account for your results. Write an equation that satisfactorily describes the decomposition.

The following test is designed to compare the lability of the ammonia in the hexaamminenickel(II) and hexaamminecobalt(III) and cobalt(II) complexes. Obtain a sample of $[Co(NH_3)_6]Cl_3$ from the chemical shelf. Add some sodium hydroxide solution to a little of the nickel (II) and cobalt (III) complexes in test tubes and cover each with a piece of moistened indicator paper. Observe what happens over several minutes and then reduce the cobalt(III) complex to cobalt(II) by adding a little aluminium powder to the alkaline solution. In which complex is the ammonia least labile?

Investigate the equilibria which are present in a solution of potassium ferrioxalate by testing separate portions with potassium thiocyanate for ferric ion and barium chloride for oxalate. What happens when an excess of a sodium oxalate or an ammonium fluoride solution is added to the ferrioxalate solution containing thiocyanate? Note your observations carefully and write equations to describe the equilibria you have found. Is ferrioxalate a labile complex?

5.4 Reference

Inorganic Experiments, Third Edition. Edited by J. Derek Woollins, 2010 WILEY-VCH Verlag GmbH&Co. KGaA, Weinheim

6 SIMULATION OF ATOMIC AND MOLECULAR ORBITALS

6.1 Purpose

Simulation of s, p and d atomic orbitals and σ, σ*, π, π* molecular orbitals. This technique gives information about the shape of the atomic and molecular orbitals.

6.2 General Information

According to the electronic state of the nucleus of an atom can not be determined precisely. In 1927, Schrödinger showed that the wave functions of a quantum mechanical system can be obtained by solving a wave equation that has since become known as the Schrödinger equation. By solving the Schrödinger equation ($H\Psi = E\Psi$), we obtain a set of mathematical equations, called **wave functions** (Ψ), which describe the probability of finding electrons at certain energy levels within an atom. A wave function for an electron in an atom is called an ***atomic orbital***; this atomic orbital describes a region of space in which there is a high probability of finding the electron. Each electron in an atom is described by four different **quantum numbers**.

The following relationships involving the first tree quantum numbers (*n*, *l*, *ml*) arise from the solution of the Schrödinger wave equation for the hydrogen atom. In this solution the values of the quantum numbers are fixed in the order listed below:

1- Principal Quantum Number (n): **Specifies the energy of an electron and the size of the orbital.**

$$n = 1,2,3,4,...$$

2- Angular Momentum (Secondary, Azimuthal) Quantum Number (l): Specifies the **shape** of an orbital with a particular principal quantum number.

$$l=0,1,2,3,...n-1$$

The secondary quantum number divides the shells into smaller groups of orbitals called **subshells** (**sublevels**). Usually, a letter code is used to identify *l* to avoid confusion with *n*:

L	0	1	2	3	4	5	...
Letter	*s*	*p*	*d*	*f*	*g*	*h*	...

3- Magnetic Quantum Number (mₗ): Specifies the **orientation in space** of an orbital of

a given energy (n) and shape (l). This number divides the subshell into individual **orbitals** which hold the electrons; there are $2l+1$ orbitals in each subshell. Thus the *s* subshell has only one orbital, the *p* subshell has three orbitals, and so on.

$$m_l=-l,-l+1,-l+2,...0,1,2,...+l$$

All orbitals with the same value of n are in the same principal electronic shell or principal level, and all orbitals with the same n and l values are in the same subshell, or sublevel.

Principal electronic shells are numbered according to the value of n. The first principal shell consists of orbitals with $n = 1$; the second principal shell of orbitals with $n = 2$; and so on. The value of n relates to the energy and most probable distance of an electron from the nucleus. The higher the value of n, the greater the electron energy and the farther, on average, the electron is from the nucleus. The principal quantum number, therefore, has a physical significance, as do the other quantum numbers. The quantum number l determines the angular distribution, or shape, of an electron and m_l determines the orientation of the orbital.

The 1*s* orbital is the lowest-energy orbital of any atom, characterized by $n = 1$, $l = m_l = 0$. It is represented by a projection of a sphere (a circle) surrounding the nucleus, within which there is a specified probability of finding the electron.

The 1*s* orbital, like all *s* orbitals, is spherically symmetrical. The 1*s* orbital contains no nodes. Because the 1*s* orbital is closest to the nucleus and has no nodes, it has the lowest energy of all the atomic orbitals (Figure 1). The second level, or shell, of electrons contains two sets of orbitals: the 2*s* and 2*p* orbitals. The 2*s* orbital, like the 1*s*, is spherically symmetrical.

All p orbitals have $l = 1$, with three possible values for $m_l = -1, 0, +1$. Therefore, there are three *p* orbitals corresponding to $m_l = 1, 0, -1$. In a useful convention, these three orbitals, which are mutually perpendicular to each other, are oriented along the three Cartesian coordinate axes and are therefore designated as p_x , p_y, and p_z. They are characterised by having one nodal plane (Figure 2).

The *p* orbital is a dumbbell-shaped region describing where an electron can be found, within a certain degree of probability. Each of these orbitals has a nodal plane.

Nodal Plane or Surface: A plane or surface associated with an orbital that defines the locus of points for which the probability of finding an electron is zero.

All d orbitals have $l = 2$, with three possible values for $m_l = -2, -1, 0, +1, +2$. Therefore, there are five *d* orbitals corresponding each these m_l values. These five magnetic quantum numbers describe the five degenerate *d* orbitals. In the Cartesian coordinate system, these orbitals are designated as d_{z2}, d_{x2-y2}, d_{xy}, d_{xz}, and d_{yz}; the last four of these *d* orbitals are characterised by two nodal planes, while the d_{z2} has surfaces of revolution (Figure 3).

Spin Quantum Number (m_s): Wave mechanics provides three quantum numbers with

which we can develop a description of electron orbitals. However, in 1925, George Uhlenbeck and Samuel Goudsmit proposed that some unexplained features of the hydrogen spectrum could be understood by assuming that an electron acts as if it spins, much like the Earth spins on its axis. There are two possibilities for electron spin (Figure 4). Thus, these two possibilities require a fourth quantum number, namely, the electron spin quantum number m_s. The electron spin quantum number may have a value of +1/2 or -1/2; the value of m_s does not depend on any of the other three quantum numbers.

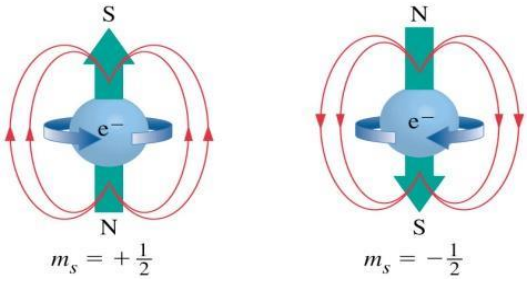

Figure 2.1: Electron spin visualised.

6.3 Procedure

This experiment describes the use of magnets to simulate *s, p* and *d* atomic orbitals from which a wide variety of molecular orbitals can be derived. The technique gives students an idea of the molecular orbitals' shape and stresses the importance of the symmetry labels.

It is well known that iron powder or iron fillings can be used to trace out the magnetic fields of magnets placed directly underneath a flat surface. A short note (see References) has described the use of such a system to simulate σ and π orbitals of *diatomic* molecules. However, this technique suffers from the major drawback that to simulate a bonding σ (1*s*) orbital, for example, two bar magnets have to be placed vertically so two *unlike* poles are in contact with the underside of the surface, *ie* N S. This is, of course, different from the bonding interaction of two atomic 1*s* orbitals where the symmetries of their wave functions have to be identical.

However, if the magnets are placed about 2 cm away from the underside of a flat aluminium disc, a different situation occurs: the iron powder, on tapping the disc gently, is found to move away from the regions where one would expect the highest magnetic field to be.

Presumably, the magnets cause the small particles of iron to become magnetised and hence align themselves in the direction of the field but, because they are all aligned in the same direction, the particles repel each other. If the permanent magnets are the correct distance from the aluminium disc, the 'magnet-iron powder' interaction will be weaker than the 'iron powder-iron powder' repulsion and hence on tapping the disc the magnetised iron particles move away from each other.

The ideal nature of this system arises from the fact that when constructing, say, a σ (1*s*) bonding orbital the 'symmetries' of the two magnetic fields under the disc have to be identical – now exactly analogous to the overlapping of two atomic 1*s* orbitals. This situation arises because of the strong repulsion between all the identically magnetised iron particles. Thus, the σ (1*s*) bonding orbital can be simulated by placing two vertical bar magnets under the disc with their poles either N N or S S. When the magnets are placed N S, a σ^* (1*s*) antibonding orbital results.

Thus, the technique not only gives the student an idea of the molecular orbital's shape but also he/she is forced to discover that those mysterious + and - signs on atomic orbitals - their symmetry labels - are very important in the bonding context. Since 1*s*, *2p* and *3d* atomic orbital representations are available, it is possible to simulate virtually any molecular orbital, the only constraint being that the molecular orbital has to be represented in only two dimensions.

6.4 Experimental

6.4.1 Materials required

The ideal magnet length is about 1-1.5 cm and it is important that they are closely matched in strength otherwise the orbital patterns become distorted. The 15 cm diametre aluminium disc used to view the magnet field patterns can be supported on a cork ring of the type used for holding round-bottomed flasks. The magnets are glued to 'Lego' pegs so that they can easily be moved about on a 'Lego' peg-board placed underneath the cork ring and yet are held firmly enough by friction so that they do not move each other by their magnetic interaction. The *d*-orbital array of magnets can be built up each time it is required but it is much more convenient to have the four (identical) magnets permanently glued together on one peg.

When constructing aromatic ring systems such as benzene or naphthalene, the peg-board has to be cut into small pieces and glued back into the required shape because the normal peg pattern does not allow hexagonal formations to be made (less satisfactorily, the magnets can be held in pieces of plasticine stuck to the bench top). The distance between the magnets in the aromatic rings, or indeed in any of the formations, depends largely on the strength of the magnets available and thus has to be determined by a little trial and error. Magnets used as carriage couplings in 'Lego' train sets are ideal.

The best way to apply the iron powder to the perfectly horizontal disc is to sprinkle it evenly from a sugar sifter. When the magnets are in position, a typist's rubber pencil is placed point down in the centre of the disc and tapped gently with a hard object until the iron powder takes up the correct shape; any disturbance of the powder distribution caused by the pencil can be rectified by careful addition of more powder from a non-magnetic spatula. However careful one is during experimentation it is soon found that the magnets collect clusters of iron filings

which tend to distort the magnetic fields; these filings can be removed by 'dabbing' the magnets with a piece of plasticine.

6.4.2 The 1s atomic orbital

Place a magnet on the peg-board with its north pole facing upwards. Put a cork ring on the peg-board so that the magnet is approximately central and cover with the aluminium disc. Sprinkle iron filings onto the disc until the central area is thinly covered. Finally, vibrate the disc by placing a typist's rubber pencil vertically at the centre and tapping the pencil top lightly with a small, hard object. The filings move away from the area of high field to leave a circular space of symmetry N (for north) which represents a *1s* orbital.

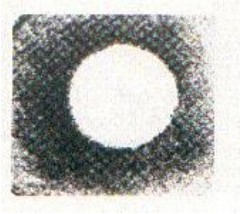

Figure 6.2: The 1s atomic orbital.

6.4.3 The 2p atomic orbital

Place two magnets upright on the peg-board so that their exposed poles are north for one magnet and south for the other. Put the cork ring and aluminium disc in place and, after sprinkling iron filings on the disc surface, tap the surface as described previously. Two clear areas develop in the iron filings, one of which has N symmetry and the other S.

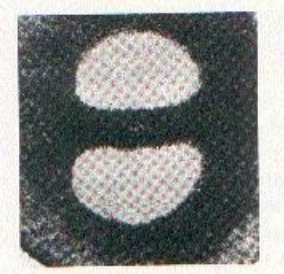

Figure 6.3: The 2p atomic orbital.

6.4.4 The 3d atomic orbital

This orbital simulation requires a group of four magnets arranged to stand upright in the form of a square so that their exposed poles alternate round the square. The developed pattern shows four equal areas of clear space among the filings which alternate in N or S symmetry and thus may be used to demonstrate a *3d* atomic orbital.

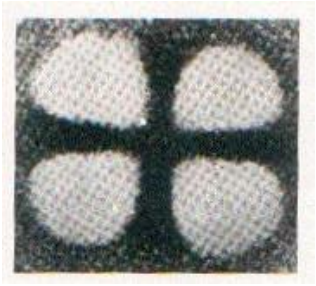

Figure 6.4: The 3d orbital.

6.4.5 Nodes

It will be noticed that the *2p* and *3d* orbital patterns have the orbital lobes separated by bands of iron filings. These bands represent nodes in the orbitals. The clear spaces in the iron filings change their N or S symmetry from one side of a node to the other in the same way that actual orbitals change the symmetry labels (+ or -) of their lobes as a nodal line or nodal plane is crossed.

The above basic magnet arrangements can now be used to investigate a variety of molecular orbital shapes in both organic and inorganic species.

6.4.6 σ (1s) orbital in H_2

Place two vertical magnets about 2.5-3.0 cm apart with their north poles uppermost and then generate the resulting magnetic pattern on the disc as described above. Repeat the experiment with one of the magnets inverted so that its south pole is uppermost; which molecular orbital does this latter pattern simulate?

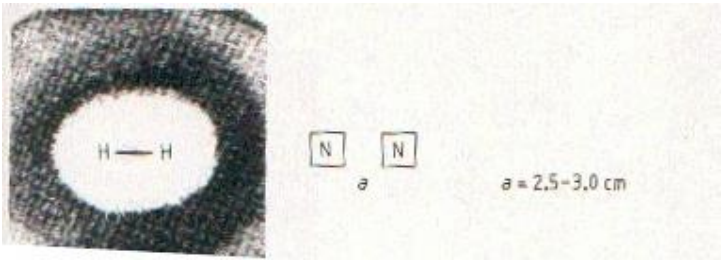

Figure 6.5: The molecular design of 1s orbital of hydrogen molecule.

6.4.7 π and π orbitals in ethene*

A π-bonding orbital in ethene, $CH_2 = CH_2$, arises from the sideways overlap of two *2p* orbitals, one on each carbon atom. Remembering that the symmetry of the interacting lobes in the *2p* orbitals have to match, decide on a suitable arrangement of vertical magnets which will mimic a bonding π -orbital. Develop the magnetic field on the aluminium disc and verify that it resembles the two lobes expected of a π-bonding orbital.

Demonstrate a π* anti-bonding orbital and convince yourself that it has the same lobal symmetry as a *3d* atomic orbital.

6.4.8 *P-O π-bonding in $OPCl_3$*

The P-O bond in phosphoryl chloride, $OPCl_3$, can be considered to involve a component which arises from an interaction between an empty phosphorus *d* orbital and a filled oxygen *2p* orbital. Demonstrate the resulting molecular orbital arising from the following magnet arrangement.

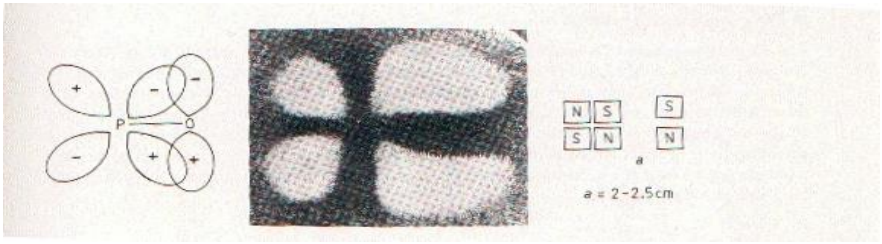

Figure 6.6: P-O bonding orbital in phosphoryl chloride.

6.4.9 *Back-bonding in transition-metal carbonyls*

It is thought that metal carbonyls such as $Cr(CO)_6$ achieve a considerable increase in stability from an interaction between filled *d* orbitals on the metal and empty π* anti-bonding orbitals on the CO ligands. The shape of the molecular orbitals resulting from this back-bonding can be illustrated by developing the magnetic field patterns using the following magnet arrangement.

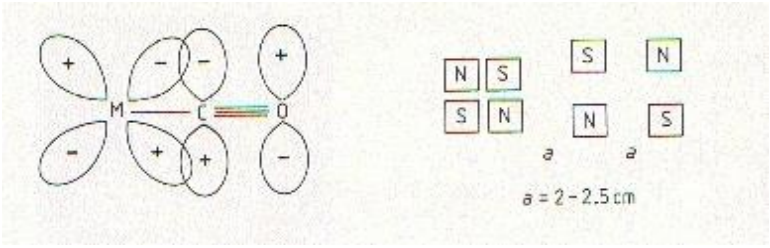

Figure 6.7: Back-bonding in transition metal carbonyl compounds.

6.4.10 *Back-bonding in transition-metal ethene complexes*

This supplementary bonding in metal ethene complexes arises from an interaction between a filled metal *d* orbital and the empty π* anti-bonding orbital of ethene in the following manner.

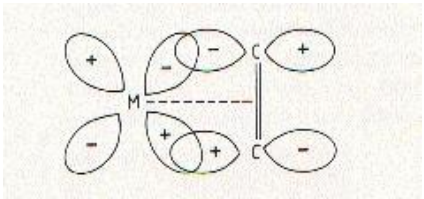

Figure 6.8: Back-bonding in transition metal-ethene complex

Deduce the correct magnet arrangement and develop the resulting magnetic field pattern.

6.4.11 *The π molecular orbitals in benzene*

The six carbon atoms in a benzene ring each have a *2p* orbital lying vertical to the plane of

the ring. Theory tells us that when *n* atomic orbitals interact in a molecule they generate *n* molecular orbitals, several of which are of high energy and are not normally occupied by electrons. Demonstrate, using six magnets placed at the corners of a regular hexagon, the shapes of the six π orbitals which occur in a benzene molecule. (Note that there is a nodal plane in the benzene π orbitals which is defined by the plane of the ring. This simulation gives only a planar, top view of the *π* orbitals; decide in each case what shape and symmetry each orbital lobe would have below the C_6 plane).

6.5 Exercises

- Write a report which is the record of how you simulate atomic and molecular orbitals, together with the schemes.
- Show the formation of bonding and antibonding orbitals (σ, σ*, π and π*) from *s* and *p* atomic orbitals.

6.6 References

1. **R.H. Petrucci**, **F. G Herring**, J.D. Madura, C. Bissonnette, **General Chemistry:** Principles and Modern Applications, Pearson Canada Inc., Toronto, Ontario, **2011**.

2. http://www.angelo.edu/faculty/kboudrea/general/quantum_numbers/Quantum_Numbers.htm

3. L.F. Druding *J. Chem. Educ.,* **1972,** 49, 617.

4. J.D. Woollins, Inorganic Experiments, VCH, Weinheim, **1994**.

7 METAL ACETYLACETONATE COMPLEXES: PREPARATION AND CHARACTERISATION

Acetylacetone (2,4-pentanedione), $CH_3COCH_2COCH_3$, is a typical β-diketone which can ionise in aqueous solution as a weak acid and famously exists in two tautomeric forms that rapidly interconvert. The pair of tautomers rapidly convert into each other and are treated as a single compound in most applications.

In pure acetylacetone, or in its solution in nonpolar organic solvents, the diketo form is in equilibrium with a cyclic enol-like form.

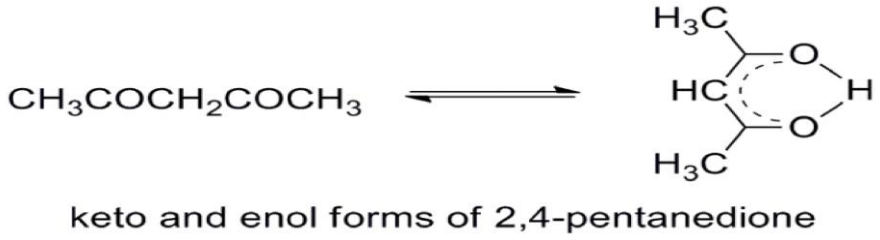

Figure 7.1: Tautomerism of acetylacetone.

In the presence of a base, 2,4-pentanedione, acacH, loses a proton and forms acetylacetonate (acac) anion, a common bidentate ligand.

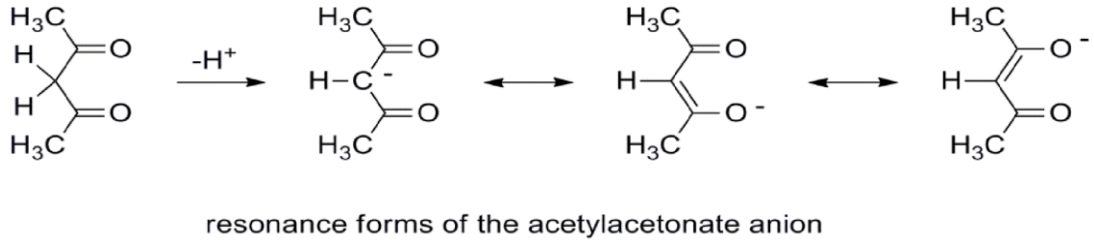

Figure 7.2: Resonance of acac anion.

The resulting anion can act as a ligand towards metal ions, forming complexes in which the ligand is usually bonded to the metal through both oxygen atoms, hence forming a six-membered ring.

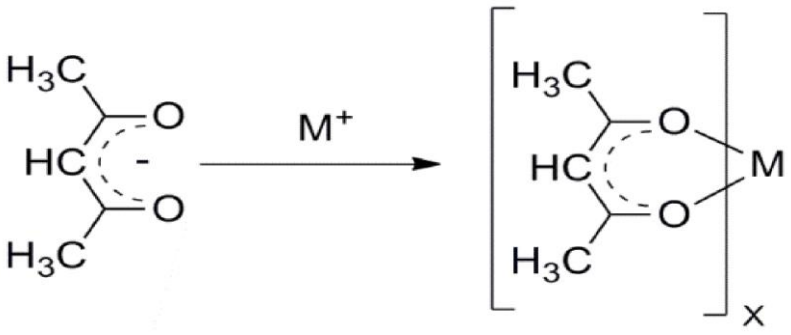

Figure 8.3: Bidentate fashion of acac ligand.

In general, the complexes isolated as crystalline solid are neutral so that a metal ion M^{x+}

forms a complex having the stoichiometry $M(CH_3COCHCOCH_3)_x$.

Figure 7.4: Stoichiometric reaction between Hacac ligand and a metal ion.

In the complexes, since the MO_2C_3 six-membered rings are planar and contain 6π electrons, they may be regarded as weakly aromatic. In $M(CH_3COCHCOCH_3)_3$ complexes the MO_6 array is octahedral, in $Cu(CH_3COCHCOCH_3)_2$ the CuO_4 group is square planar and in $VO(CH_3COCHCOCH_3)_2$, the VO_5 group is square pyramidal.

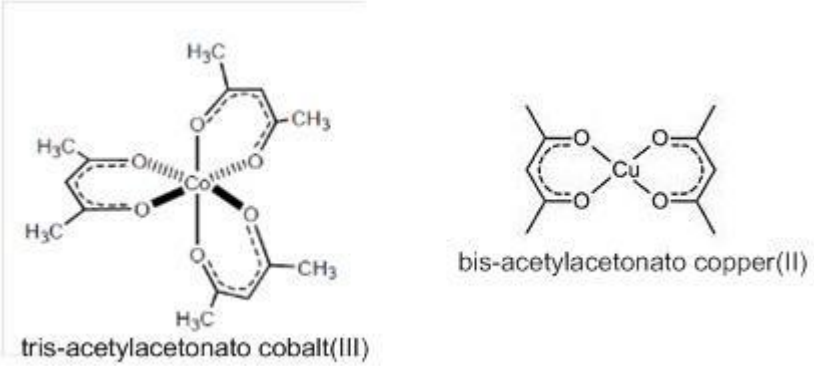

Figure 7.5: Structure of tris- and bis-acac complexes.

Acetylacetonate complexes are soluble in organic solvents, in contrast to the related metal halides. Because of these properties, acac complexes are sometimes used as catalyst precursors and reagents.

In this experiment, you will prepare and purify several metal acetylacetonate complexes. You will also interpret ^1H and ^{13}C NMR spectra of complexes.

7.1 Metal Acetylacetonates

7.1.1 Al^{3+} Complex

Weigh, into a 100 cm^3 conical flask, 3 g of acetylacetone, using a dropping pipette to transfer the liquid into the flask. Add 40 cm^3 distilled water followed by 8 cm^3 of 5 mol dm^{-3} ammonia solution. Dissolve 3 g of aluminium sulphate $[Al_2(SO_4)_3.16H_2O]$ in 30 cm^3 cold distilled water. To the almost clear solution add the ammoniacal acetylacetone solution in portions with shaking. After complete addition of the acetylacetone, check the pH using blue litmus paper and, if the solution is still acidic, add further small portions of 5 mol dm^{-3} ammoniacal solution until it is neutral to litmus. Allow to stand for 15 minutes. Filter off the cream coloured product at the water pump, wash with 100 cm^3 of cold distilled water and suck dry for 10 minutes. Transfer the dry product to a weighed sample tube and dry in a vacuum desiccator over anhydrous $CaCl_2$. Weigh the dry product and calculate the percentage yield.

Figure 7.6: Formation of the Al(acac)$_3$ complex.

Recrystallise a small sample (0.5 g) from cyclohexane. The resulting needles should be filtered at the water pump, washed with a little cold cyclohexane, and sucked dry for 15 minutes. Record the melting point.

7.1.2 VO^{2+} complex

Place 2.5 mL distilled water in a 25 mL round-bottomed flask and slowly add to it an equal volume of concentrated H_2SO_4. Then add 6 mL of ethanol followed by 1.25 g vanadium(V) oxide, V_2O_5. Add a water-cooled vertical condenser and reflux this mixture for about 1.5 hours using a heating mantle. The solution will turn a dark blue-green colour. Cool the mixture and filter using a small plug of glass wool, discarding any solid residue. Add 3 mL of acetylacetone dropwise to the filtrate with stirring. Neutralise the mixture by adding it carefully to a solution 10 g of anhydrous Na_2CO_3 in 75 mL distilled water, contained in a 250-mL beaker, while stirring the mixture using a magnetic stirrer. The resulting mixture should then be cooled in ice water for 15 minutes before vacuum filtering. Wash the dark green product with cold distilled water (2 x 5 mL). Suck dry under vacuum for 15 minutes, then dry in a vacuum desiccator over anhydrous $CaCl_2$. Weigh the dried product and calculate the percent yield.

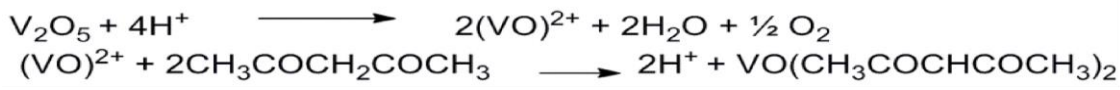

Figure 7.7: Formation of VO(acac)$_2$ complex.

7.1.3 Cr^{3+} complex

Weigh 0.7 g of chromium(III) chloride hexahydrate ($CrCl_3.6H_2O$) directly into a 100-mL erlenmeyer flask and dissolve it in 25 mL of distilled water. Weigh out 5 g of urea and add it in 3 or 4 portions to the deep green chromium solution, stirring well after each addition. Then add 1.75 mL of acetylacetone dropwise, using a pipette. Clamp the flask in a boiling water bath and heat the mixture while stirring for approximately one hour. The solution should initially be very dark and almost black in appearance, but as the reaction proceeds, deep maroon plate-like crystals form as a crust on the surface of the reaction mixture.

Cool the reaction mixture and vacuum-filter the product. Do not wash the product with water. Dry it in air. Weigh the dried product and calculate the percent yield.

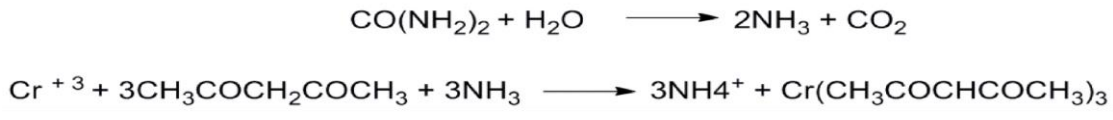

Figure 7.8: Formation of Cr(acac)$_3$ complex.

The urea undergoes slow hydrolysis, liberating ammonia, which then controls the pH of the reaction mixture.

7.1.4 Fe^{3+} complex

Dissolve 3.3 g of finely-ground iron(III) chloride hexahydrate ($FeCl_3.6H_2O$) in 25 mL of distilled water in a 100-mL beaker. Add, over a period of 15 minutes, a solution of 3.8 mL of acetylacetone in 10 mL of methanol. Stir whilst the addition using a magnetic stirrer. Add to the resulting blood-red mixture, over a period of 5 minutes, a solution of 5.1 g of sodium acetate in 15 mL of distilled water, maintaining the stirring throughout the process. At this point, a red crystalline solid should precipitate. Heat the whole mixture rapidly to about 80°C on a hot plate. Monitor the temperature carefully with a thermometre and maintain this temperature for 15 minutes while rapidly stirring. Cool to room temperature with a water bath and then cool further in an ice bath. Vacuum-filter the product and wash with 10 mL of cold distilled water. Dry with vacuum for 15 minutes. Then dry in a vacuum desiccator over anhydrous $CaCl_2$. Weigh the dry product and calculate the percent yield.

$$Fe^{+3} + 3CH_3COCH_2COCH_3 \longrightarrow 3H^+ + Fe(CH_3COCHCOCH_3)_3$$

$$3H+ + 3CH_3COO^- \longrightarrow 3CH_3COOH$$

Figure 7.9: Formation of the $Fe(acac)_3$ complex.

7.1.5 Co^{3+} complex

Weigh into a 100-mL beaker 0.38 g of cobalt carbonate and add 3 mL of acetylacetone. Heat the mixture to about 90°C on a hot plate with continuous stirring. Monitor the temperature carefully with a thermometre. While maintaining the temperature around 90°C, add dropwise 4.5 mL of a 10% solution using a dropping pipette. Cover the flask with a watch glass between hydrogen peroxide additions. The whole addition of the hydrogen peroxide solution should occupy about 30 minutes. Stirring should be maintained throughout the addition and then for a further 15 minutes. Cool in an ice-water bath for 30 minutes. Vacuum-filter the dark green product. Vacuum dry for 15 minutes and then dry in an oven at 110°C. Weigh the dry product and record the percent yield.

7.1.6 Cu^{2+} complex

To a solution of 2 g of copper(II) chloride dihydrate ($CuCl_2.2H_2O$) in 12 mL of distilled water in a 250-mL beaker, add dropwise over a period of 20 minutes a solution of 2.5 mL of acetylacetone in 5 mL of methanol, while maintaining constant stirring. Add to the resulting mixture 3.5 g of sodium acetate in 8 mL of distilled water over a period of 5 minutes. Heat the

mixture to 80ºC in a hot plate for 15 minutes, still maintaining rapid stirring. Monitor the temperature carefully with a thermometre. Cool to room temperature and then place in an ice water bath. Filter off the blue-gray product and wash with ~50 mL of cold distilled water and vacuum dry for 15 minutes before drying in an oven at 110ºC. Weigh the dry product and record the percent yield.

$$Cu^{2+} + 2CH_3COCH_2COCH_3 \longrightarrow 2H^+ + Cu(CH_3COCHCOCH_3)_2$$

$$H^+ + CH_3COO^- \longrightarrow CH_3COOH$$

Figure 7.10: Formation of $Cu(acac)_2$ complex.

7.2 Nuclear Magnetic Resonance Spectra of Acetyl Acetonates

In this section the, ^1H and ^{13}C NMR spectra of one diamagnetic metal acetylacetonate, $Al(CH_3COCHCOCH_3)_3$ and of acetylacetone itself are examined and assigned.

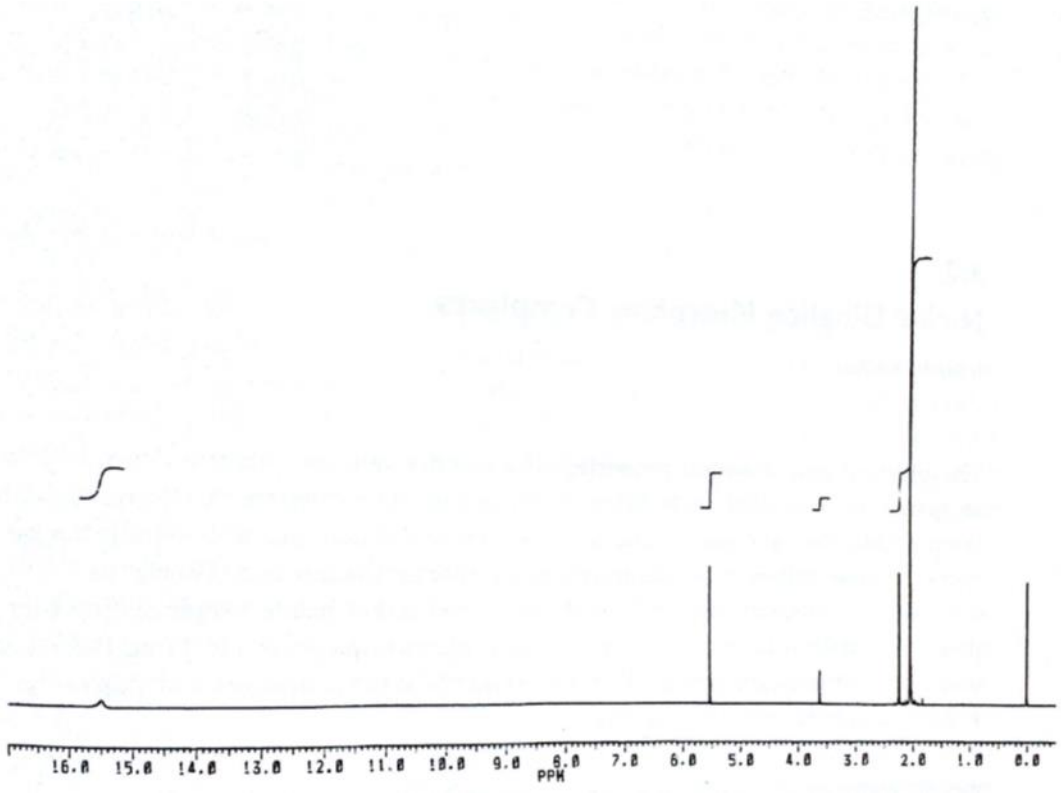

Figure 7.11. The ^1H NMR spectrum of $CH_3COCH_2COCH_3$ containing both keto and enol forms.

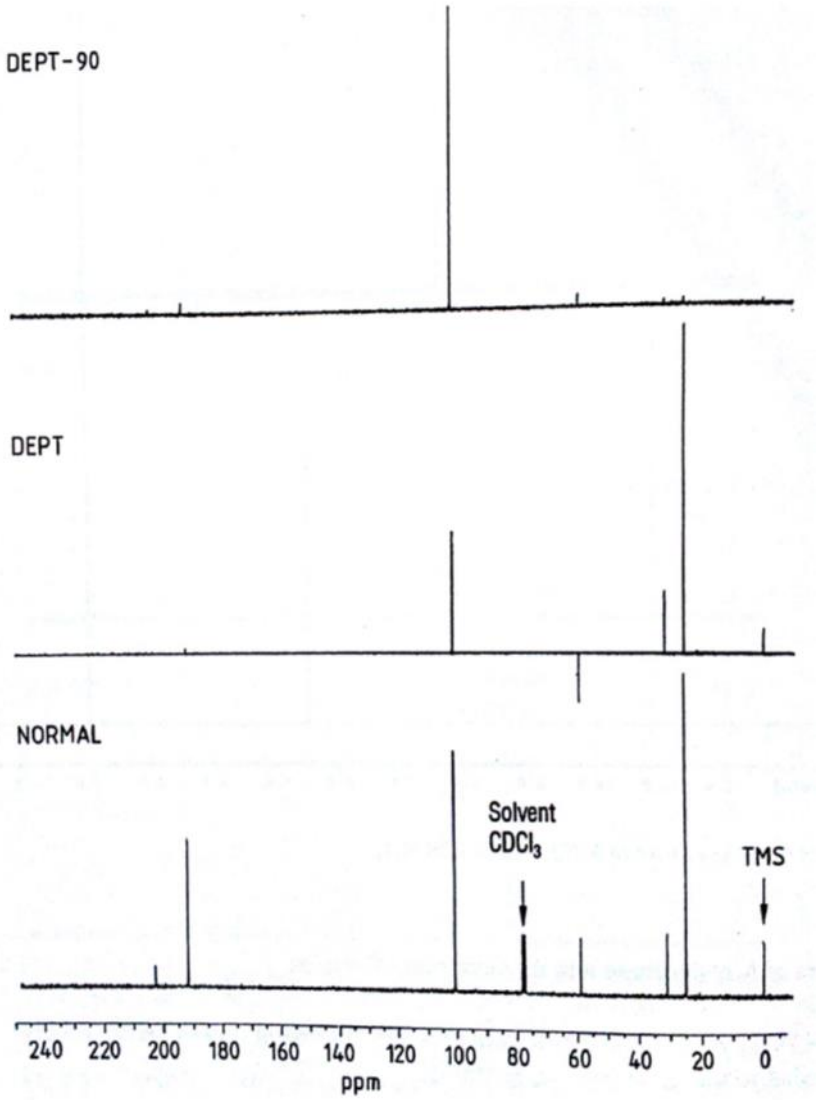

Figure 7.12. The ^{13}C NMR spectrum of $CH_3COCH_2COCH_3$ containing both keto and enol forms.

In acetylacetone itself, both keto and enol forms are present. Since the enol form can be regarded as a complex of H^+, its ^1H and ^{13}C NMR spectra may be expected to show similarities with those of the aluminium complex.

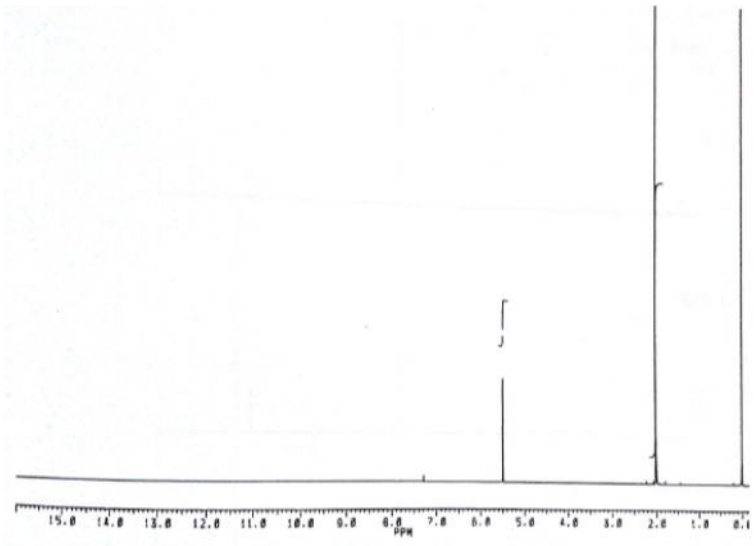

Figure 7.13. The ^{1}H NMR spectrum of $Al(CH_3COCHCOCH_3)_3$

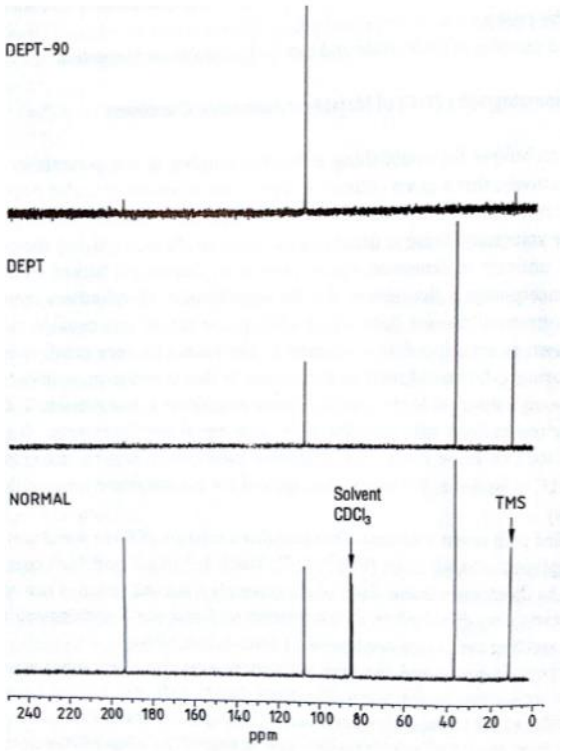

Figure 7.14. The ^{13}C NMR spectrum of $Al(CH_3COCHCOCH_3)_3$.

Reference: J.D. Woollins, Inorganic Experiments, VCH, Weinheim, 1994.

8 SPECTROPHOTOMETRIC DETERMINATION OF THE COMPOSITION OF A COORDINATION COMPLEX IN SOLUTION

8.1 Ultraviolet-Visible (UV-Vis) Spectroscopy

Electromagnetic radiation such as visible light is commonly treated as a wave phenomenon, characterised by a wavelength or frequency. Wavelength is defined as the distance between adjacent peaks (or troughs), and may be designated in metres, centimetres or nanometres (10^{-9} metres). Frequency is the number of wave cycles that travel past a fixed point per unit of time, and is usually given in cycles per second, or hertz (Hz).

The energy levels of atoms and molecules are quantized, i.e. there are discrete energy levels in atoms and molecules (Figure 8.1).

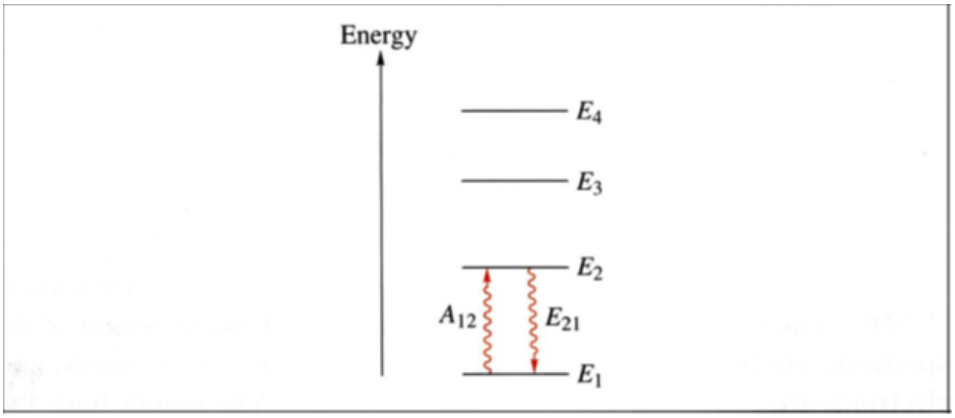

Figure 8.1. Discrete energy levels of an atom or molecule.

E_1 corresponds to the ground state of the atom/molecule, and E_2, E_3 and E_4 represent excited states. Given that these are all discrete energy levels, the difference in energy between them (and so the energy required for a particular transition) will also be a discrete value, which is called a quantum. We can see from Figure 1 that in order to excite the atom/molecule from E_1 to E_2 it must absorb an amount of energy equivalent to A_{12}. Excited states are generally short lived and relax back to the ground state by emission of energy, in this case E_{21}. The energy difference between the excited state (E_2) and the ground state (E_1) will correspond to a certain frequency(ν) or wavelength (λ) of electromagnetic radiation, and this will depend upon the type of transition (and hence the separation between energy levels). The relationship between the energy of a transition and the frequency is given by equation (1):

$$\Delta E = h\nu \tag{1}$$

and so:

$$\Delta E = \frac{hc}{\lambda} \tag{2}$$

The energy of a particular transition is, therefore, proportional to the frequency and wavelength.

The electromagnetic spectrum is divided into regions. The names of these regions and the associated together with the corresponding energies, wavenumbers, are shown in Figure 8.2.

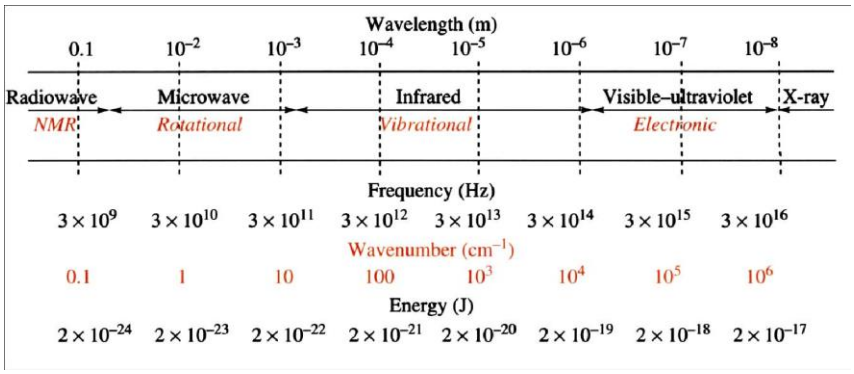

Figure 8.2. The electromagnetic spectrum.

The UV-Vis region is important, since absorptions in this region give rise to the colour associated with molecules; Figure 8.3 shows this region in more detail.

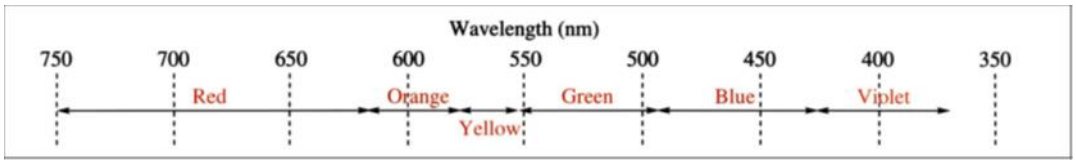

Figure 8.3. The visible region of the electromagnetic spectrum.

The term UV-Vis normally applies to radiation with a wavelength in the range 200-800 nm. There are many groups that absorb below 200 nm, but this part of the spectrum is difficult to examine (as oxygen absorbs UV radiation below 200 nm) unless the spectra are recorded in a vacuum (vacuum UV-Vis).

8.2 UV-Vis absorption bands

The difference between electronic energy levels is greater than the difference between any other molecular energy levels, so these transitions require the higher energy of short wavelength radiation. Promotion between other energy levels, i.e. vibrational or rotational,

requires only the lower energy infrared (vibrational) or microwave (rotational) radiation (Figure 4). At room temperature, the majority of molecules are in the lowest vibrational state of the lowest electronic energy level, the "ground state" (E_1). Absorption of UV or visible light leads to promotion of an electron from E_1 to the excited electronic level, E_2. The electronic transition is accompanied by vibrational and rotational transitions, so that the promotion of an electron can occur from the ground state electronic energy level of E_1 to any of the vibrational or rotational energy levels of E_2. This explains why UV-Vis absorption bands are characteristically broad, although energy transitions between rotational and vibrational energy levels within one electronic energy level can show fine structure.

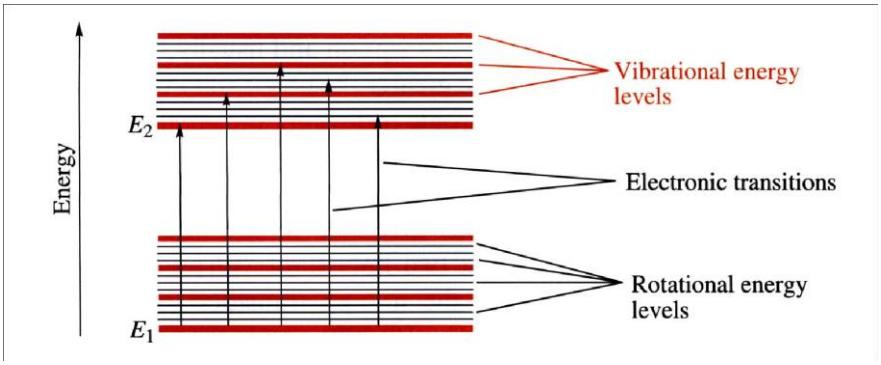

Figure 8.4. Schematic diagram showing possible molecular electronic transitions, and vibrational and rotational energy levels.

The fact that there are many electronic transitions possible, however, does not mean that they can or will occur. There are complex selection rules (spin and symmetry selection rules) based on the symmetry of the ground and excited states of the molecule under examination. However, the so-called "forbidden" transitions can still occur, but give rise to weak absorptions.

According to the Beer-Lambert law, the absorbance, A, of a solution is directly proportional to the path length (l, length of the cell containing the solution, in cm) and the concentration of the absorbing molecule (c, in moles per litre), according to equation (3):

$$A = \epsilon c l \tag{3}$$

where ε= molar absorptivity, A= absorbance, c= concentration (M), l = cell length (cm)

Usually, energy absorption is reported as molar absorptivity (also called molar extinction coefficient) rather as the actual absorbance. The magnitude of ε reflects both the size of the chromophore and the probability that light of a given wavelength will be absorbed when it strikes the chromophore.

8.3 Terminology

Chromophore: A covalently unsaturated group responsible for electronic absorption. or Any group of atoms that absorbs light whether or not a colour is thereby produced. e.g. C=C, C=O, NO_2 etc. A compound containing chromophore is called chromogen.

Auxochrome: A saturated group with non-bonding electron when attached to chromophore alters both wavelengths as well as intensity of absorption. e.g. OH, NH_2, NHR etc.

Bathochromic group: The group which deepens the colour of chromophore is called bathochromic group. e.g. Primary, secondary and tertiary amino groups.

Bathochromic shift: (Red shift) shift of lambda max (λ_{max}) to longer side or less energy is called bathochromic shift or read shift. This is due to substitution or solvent effect.

Hypsochromic shift: (Blue shift) shift of lambda max (λ_{max}) to shorter side and higher energy is called hypsochromic or blue shift. e.g., solvent effect.

Hyperchromic effect: an increase in absorption intensity.

Hypochromic effect: a decrease in absorption intensity.

8.4 Electronic Transitions

Absorption of UV or visible light results in electronic transitions; an electron is promoted from an occupied molecular orbital (usually a non-bonding n or bonding π orbital) to an unoccupied molecular orbital (an antibonding π* or σ* orbital) of greater potential energy.

As a rule, energetically favoured electron promotion will be from the highest occupied molecular orbital (HOMO) to the lowest unoccupied molecular orbital (LUMO), and the resulting species is called an excited state. The four important transitions and their relative energies are given in Figure 8.5.

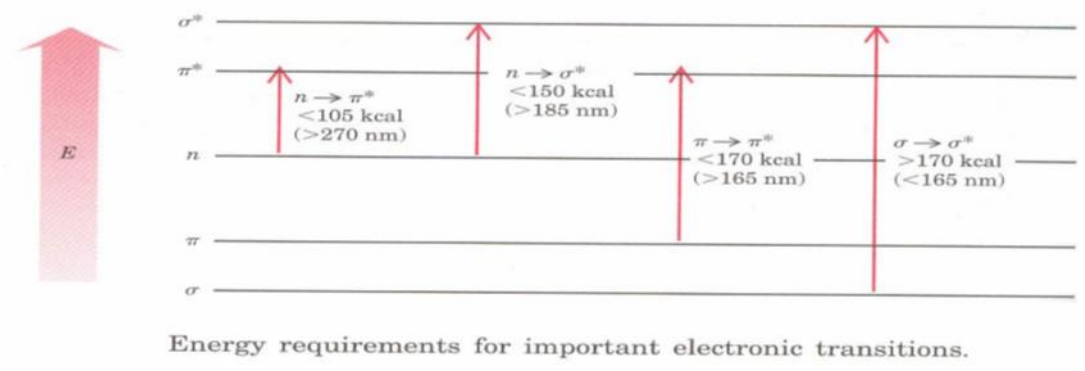

Figure 8.5. The four important transitions and their relative energies.

*8.4.1 σ to σ * Transitions*

An electron in a bonding s orbital is excited to the corresponding antibonding orbital. The energy required is large. For example, methane (which has only C-H bonds, and can only undergo σ to σ * transitions) shows an absorbance maximum at 125 nm. Absorption maxima due to σ to σ * transitions are not seen in typical UV-Vis.

*8.4.2 n to σ * Transitions*

Saturated compounds containing atoms with lone pairs (nonbonding electrons) are capable of n to σ * transitions. These transitions usually need less energy than n to σ * transitions. They can be initiated by light whose wavelength is in the range 150 – 250 nm. The number of organic functional groups with n to σ * peaks in the UV region is small.

*8.4.3 n to π * and π to π * Transitions*

Most absorption spectroscopy of organic compounds is based on transitions of n or π electrons to the π * excited state. This is because the absorption peaks for these transitions fall in an experimentally convenient region of the spectrum (200 - 700 nm). These transitions need an unsaturated group in the molecule to provide the π electrons. Molar absorptivities from n - π* transitions are relatively low, and range from 10 to100 L mol^{-1} cm^{-1}. π - π * transitions normally give molar absorptivities between 1000 and 10,000 L mol^{-1} cm^{-1}.

Absorption range for various electronic transitions is given in Figure 8.6.

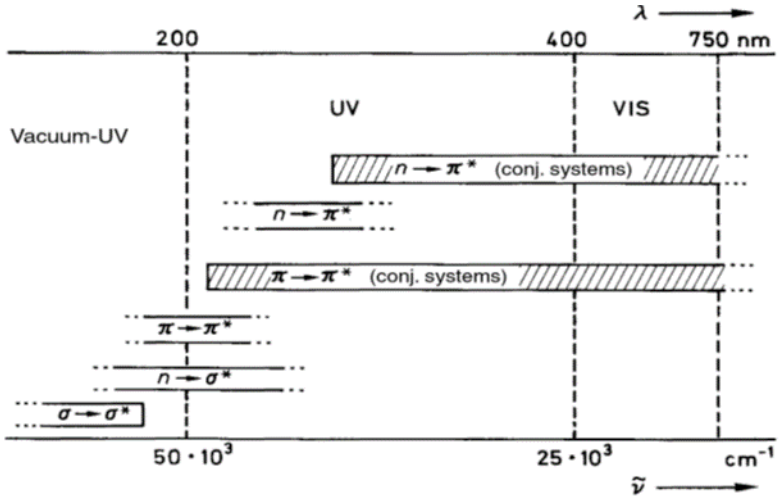

Figure 8.6. Absorption range for various electronic transitions.

8.5 Job's Method

Several techniques have been developed for the determination of the stoichiometry of chemical

equilibrium reactions, including the method of continuous variation, slope ratio method, and mole ratio method, to name a few. Due to its simplicity, the method of continuous variation (often referred to as Job's method), first described by Ostromisslensky, Dension, and Job, is widely regarded as the most popular of these methods.

$$nA + mB \quad A_nB_m \qquad (4)$$

where A and B represent the free species at equilibrium (i.e., a ligand and a substrate), and A_nB_m represents a molecular complex of A and B.

In this method, the measured concentration of the complex A_nB_m (or a parameter that is proportional to its concentration, such as its UV/vis or infrared absorbance or the integrated NMR signal intensity) is plotted against the mole fraction of one reactant while the sum of the reactant concentrations, c_{0SUM}, is kept constant. This plot is referred to as a Job plot. It follows from eq 4 that $c_{0A} = c_A + nc_AnB_m$ and $c_{0B} = c_B + mc_AnB_m$, where c_A, c_B, and c_AnBm refer to the species present in solution, while c_{0A} and c_{0B} refer to the total concentration of reactants A and B, respectively. The latter are related to c_{0SUM} at any given mole fraction f of species A by

$$c_A^0 = f \times c_{\mathrm{SUM}}^0 \qquad (5)$$

$$c_B^0 = (1-f) \times c_{\mathrm{SUM}}^0 \qquad (6)$$

For association equilibria of this type, the highest concentration of the complex A_nB_m and, thereby, the maximum in the Job plot is given by

$$x = \frac{n}{(n+m)} \qquad (7)$$

where x is the mole fraction of A at the maximum point of the curve. Clearly, this relationship makes Job's method an extremely powerful tool to determine the stoichiometries of equilibrium.

In Job's method, different amounts of stock solutions of A and B are mixed, varying the mole ratio of reactants in such a compensatory manner that their total molar concentration is kept constant. The absorbances of these solutions are then measured at a fixed wavelength, and plotted as a function of mole fraction of ligand, or of metal. The position of maximum absorbance on this plot, in relation to the mole-fraction axis, gives the stoichiometry of the complex.

If a single, stable complex, one which is not appreciably dissociated, is formed, a plot of absorbance vs mole fraction of reactant gives a characteristic triangular plot. The mole fraction of the maximum of this plot, the apex of the triangle, indicates the composition of the complex. However, if a weak complex is formed, a very curved plot results. Cognizance of the inherent limitations of the continuous variations method in studying complexes formed in solution is necessary before attempting to determine the composition of the complex formed. The valid data are obtained by the continuous variations method only when there is one predominant

complex formed and the reactants and complex are not involved in concomitant equilibria.

8.6 Experimental

8.6.1 Determination of the Composition of Fe+3- Salicylic Acid Complex

Prepare 500 mL $2x10^{-3}$ M ammonium iron(III) sulfate and 500 mL 2 x 10^{-3} M salicylic acid solutions in 2 x 10^{-3} M HCl solution. Obtain a set of working solutions by mixing stock ligand and metal solution according to the following table.

Fe^{+3} Solution (mL)	1	2	3	4	5	6	7	8	9
Salicylic Acid Solution (mL)	9	8	7	6	5	4	3	2	1

Choose the appropriate wavelength by taking the spectra (350-700 nm) of the stock solutions and one of the working solution. Determine the absorbance of working solutions at this wavelength. Present the absorbance of each mixture and the mole fraction of metal in each mixture in a table. From this table, construct a Job's plot of absorbance (vertical axis) versus mole fraction of metal. Triangulate the plot and determine the formula of the Fe^{+3}- Salicylic acid complex from the mole fraction of maximum absorbance.

8.7 References

1- R. J. Anderson, D. J. Bendell, P.W. Groundwater, Organic Spectroscopic Analysis, Royal Society of Chemistry, 2004.

2- E. J. Olson, P. Bühlmann, J. Org. Chem. 2011, 76, 8406–8412.

3- P. MacCarthy, Anal. Chem. 1978, 50, 2165.

4- A. Facchiano, R. Ragone, Analytical Biochemistry 2003, 313, 170–172.